THE ASTROPHYSICAL JOURNAL, 473:322–342, 1996 December 10

THE SOFT GAMMA REPEATERS AS VERY STRONGLY MAGNETIZED NEUTRON STARS. II. QUIESCENT NEUTRINO, X-RAY, AND ALFVÉN WAVE EMISSION

CHRISTOPHER THOMPSON[1]
Canadian Institute for Theoretical Astrophysics, Toronto, Canada
AND
ROBERT C. DUNCAN
Department of Astronomy, University of Texas, Austin, TX 78712
Received 1995 August 15; accepted 1996 June 10

ABSTRACT

We calculate the quiescent X-ray, neutrino, and Alfvén wave emission from a neutron star with a very strong magnetic field, $B_{\rm dipole} \sim 10^{14}$–$10^{15}$ G and $B_{\rm interior} \sim (5–10) \times 10^{15}$ G. These results are compared with observations of quiescent emission from the soft gamma repeaters and from a small class of anomalous X-ray pulsars that we have previously identified with such objects. The magnetic field, rather than rotation, provides the main source of free energy, and the decaying field is capable of powering the quiescent X-ray emission and particle emission observed from these sources. New features that are not present in the decay of the weaker fields associated with ordinary radio pulsars include fracturing of the neutron star crust, strong heating of its core, and effective suppression of thermal conduction perpendicular to the magnetic field. As the magnetic field is forced through the crust by diffusive motions in the core, multiple small-scale fractures are excited, as well as a few large fractures that can power soft gamma repeater bursts. The decay rate of the core field is a very strong function of temperature and therefore of the magnetic flux density. The strongest prediction of the model is that these sources will show no optical emissions associated with X-ray heating of an accretion disk.

Subject headings: gamma rays: bursts — stars: magnetic fields — stars: neutron — X-rays: stars

1. INTRODUCTION

The dipole magnetic fields of young radio pulsars, as inferred from their observed spin-down rates, lie in a relatively narrow range: $5 \times 10^{11} \lesssim B_{\rm dipole} \lesssim 2 \times 10^{13}$ G for pulsars whose spin-down age is less than $\sim 10^6$ yr (see, e.g., Kulkarni 1992). Although this observational fact is well established, the existence of neutron stars with stronger magnetic fields remains very much a possibility. The detection of white dwarfs with fields as large as $\sim 5 \times 10^8$ G (which would correspond to $B \sim 10^{14}$ G if the star were compressed to nuclear matter density) demonstrates that even quiescent, liquid stars can maintain strong magnetic fields. Thus, the tensile strength of a neutron star's crust does not fundamentally limit the magnetic field that the star can support. Because a neutron star born with $B_{\rm dipole} \gtrsim 10^{14}$ G spins down rapidly, it passes the radio death line much faster than does an ordinary radio pulsar (Duncan & Thompson 1992, hereafter DT92). When combined with the relatively small radio beaming angles of long-period pulsars (see, e.g., Kulkarni 1992), this implies a strong observational bias against detecting the radio pulsations from such a *magnetar*.

What are alternative strategies for searching for magnetars? A key point is that as $B_{\rm dipole}$ increases, the ratio of the magnetic energy to the rotational energy of the neutron star also increases. There is, in particular, a characteristic age at which the exterior magnetic dipole energy begins to dominate the rotational energy:[2]

$$t_{\rm mag} \sim 400\left(\frac{B_{\rm dipole}}{10B_{\rm QED}}\right)^{-4} \text{ yr} . \tag{1}$$

Since the *total* magnetic energy of the star is probably much greater than the exterior dipole component, it will exceed the rotational energy even earlier. When combined with the fact that the decay time of the core magnetic field decreases rapidly with flux density (see, e.g., Thompson & Duncan 1993b, hereafter TD93b), this implies that the dominant source of free energy in a magnetar is not the rotation, but the magnetic field itself. Indeed, the decaying field can keep the core and surface of the neutron star much hotter than standard cooling models would suggest (TD93b). The Maxwell stresses that develop as the magnetic field diffuses through the core are large enough to fracture the rigid crust of the neutron star. If the scale of the fracture is comparable to the thickness of the crust, then $\sim 10^{41}$ ergs is injected into the magnetosphere, with a radiative signature (we have argued) that is similar to a soft gamma repeater burst (Thompson & Duncan 1995, hereafter TD95).

Several independent arguments identify the soft gamma repeater source SGR 0526−66 as a neutron star with $B_{\rm dipole} \sim 6 \times 10^{14}$ G and an internal magnetic field approximately 1 order of magnitude larger (TD95). The strongest evidence comes from an extremely energetic ($\Delta E \sim 5 \times 10^{44}$ ergs) and prolonged ($\Delta t \gtrsim 200$ s) burst emitted by that source on 1979 March 5. (For a review of this source, see Cline 1982, and for the SGR sources in general, see Norris et al. 1991.) The very strong magnetic field can (1) spin down the star to an 8 s period (as exhibited by the 1979 March 5 burst) in the 5×10^3 yr age (Vancura et al. 1992) of the surrounding LMC supernova remnant N49; (2) provide sufficient energy to power the March 5 event; (3) undergo a

[1] Current address: Physics and Astronomy, University of North Carolina CB3255, Chapel Hill, NC 27599.

[2] Here $B_{\rm QED} = m_e^2 c^3/e\hbar = 4.4 \times 10^{13}$ G.

large-scale interchange instability whose growth time is comparable to the ~ 0.2 s width of the initial hard transient phase of the March 5 event; (4) confine the energy that was radiated in the soft tail of that burst; and (5) reduce the Compton scattering cross section sufficiently to generate a radiative flux that is $\sim 10^4$ times the (nonmagnetic) Eddington flux (Paczyński 1992).

There are two additional reasons for considering a strong magnetic field, which we will focus on in this paper (see Thompson & Duncan 1993b, hereafter TD93b and TD95 for a preliminary discussion): (6) The field can decay significantly in $\sim 10^4$–10^5 yr, as is required to explain the activity of SGR 0526−66 (and also SGR 1806−20) on this timescale; and (7) by heating the interior of the neutron star, the field can power the quiescent X-ray emission ($L_X \sim 7 \times 10^{35}$ ergs s^{-1}) observed by *Einstein* and *ROSAT* (Rothschild et al. 1993; Rothschild, Kulkarni, & Lingenfelter 1994).

A second soft gamma repeater source, SGR 1806−20, has been convincingly identified with a quiescent X-ray source discovered by *ASCA* of luminosity $L_X \sim 3 \times 10^{34}(D/8\ \mathrm{kpc})^2$ ergs s^{-1} (Murakami et al. 1994). The spin period of this source is not known, although there is marginal evidence for a 2.8 s periodicity from the summed light curves of the bursts (Ulmer et al. 1993). Like SGR 0526−66, this repeater is associated with a supernova remnant (G10.0−0.3) of age $\sim 10^4$ yr (Kulkarni et al. 1994). Unlike the LMC remnant N49, which contains SGR 0526−66, the nonthermal radio emission of G10.0−0.3 is strongly peaked about the X-ray source down to arcsecond scales (Vasisht, Frail, & Kulkarni 1995). The particle luminosity required to power this radio emission is $\sim 5 \times 10^{36} \times (D/8\ \mathrm{kpc})^{2.5}$ ergs s^{-1} (Appendix A). We will show that the decay of a strong magnetic field can power not only surface X-ray emission but also a steady stream of low-amplitude Alfvén waves into the magnetosphere. This provides a new mechanism, in addition to unipolar induction, for powering a quasi-steady relativistic particle flux from a neutron star.

The third known soft gamma repeater, SGR 1900+14, has a possible identification with SNR G42.8+0.6 (Vasisht et al. 1994), although the association is less certain because the Network Synthesis error box (Hurley et al. 1994b) lies outside the remnant.

In this paper, we will also focus on a small class of anomalous X-ray pulsars, the best studied of which is 1E 2259+586 (Gregory & Fahlman 1980). This object shares a number of properties with SGR 0526−66 in its quiescent state (Thompson & Duncan 1993a, hereafter TD93a; TD93b; Corbet et al. 1995). More generally, these sources have the following characteristics (Mereghetti & Stella 1995; Duncan & Thompson 1995, hereafter DT95): spin periods of several seconds, association with SNRs of age $\sim 10^4$ yr, and soft X-ray emission at a level of $L_X \sim 10^{35}$–10^{36} ergs s^{-1}.

In sum, one must entirely rethink the physics of neutrino cooling, photon emission, and particle emission from a neutron star, when its magnetic field (instead of its rotation) is the main source of free energy.

Our purpose in this paper is threefold. First, the relative merits of accretion versus magnetic field decay as the energy source for the quiescent X-ray emission of the soft gamma repeater (SGR) and anomalous X-ray pulsar (AXP) sources are discussed in § 2. Second, the physical mechanisms by which an (internal) magnetic field stronger than $\sim 10^2 B_{\mathrm{QED}} = 4.4 \times 10^{15}$ G decays in a neutron star are then investigated in some detail. We explain in § 3.1 why a rigid crust is not needed to achieve (temporary) hydromagnetic stability. Some subtleties associated with ambipolar diffusion of a magnetic field in the core are discussed in § 3.2, and the balance between frictional heating and neutrino cooling is calculated in § 3.3. When a magnetic field stronger than $\sim 10^{14}$ G is dragged through the crust by the diffusive motions in the core, Hall turbulence is excited, which leads to multiple small-scale fractures (§ 3.4). A fraction of the crustal field energy is converted to larger scale fractures (of size comparable to the crustal thickness) that release enough energy to power SGR bursts (§ 3.5). A distinctive feature of the internal heating of the neutron star is a quiescent surface X-ray glow (§ 3.6), whose maximum luminosity is $\sim 10^{35}$–10^{36} ergs s^{-1} at an age of $\sim 10^4$ yr. Anisotropic thermal conduction in the magnetized core (§ 3.7) may impart inhomogeneities to the surface X-ray flux and will also keep part of the core thermally disconnected from both a kaon condensate in the central core (§ 3.8) and from the surface. The main effect of neutron superfluidity is to *increase* the equilibrium core temperature and surface temperature (§ 3.8). Our third and final task is to compare the predicted observational signatures of a magnetar in its quiescent state with observations of the SGR and AXP sources (§ 4). The observational effects of glitches in terms of variability of the quiescent X-ray luminosity are outlined in § 4.2. We present our conclusions in § 5.

2. ARE X-RAYS POWERED BY ACCRETION OR MAGNETIC FIELD DECAY?

2.1. *Soft Gamma Repeaters*

The rotational energy of SGR 0526−66 is far too small to power its quiescent X-ray emission of $\sim 7 \times 10^{35}$ ergs s^{-1}. At the estimated age of $\sim 5 \times 10^3$ yr (Vancura et al. 1992), the maximum luminosity derivable from spin-down is

$$L_X \sim \frac{1}{2t} I \left(\frac{2\pi}{P}\right)^2 \sim 2 \times 10^{33}\ \mathrm{ergs\ s^{-1}}\,, \qquad (2)$$

where I is the moment of inertia of the neutron star. Accretion is therefore the most obvious energy source for the quiescent X-ray emission detected from the SGR sources, but there are a number of difficulties with this interpretation:

1. SGR 0526−66 appears to have a large proper motion $V_\perp = 1200 \pm 300$ km s^{-1}, based on the position of the quiescent *Einstein* and *ROSAT* source (DT92; Rothschild et al. 1994). Such a proper motion is inconsistent with the neutron star remaining in a tight binary (DT92; Brandt & Podsiadlowski 1995).

2. If the radio plerion surrounding SGR 1806−20 (Kulkarni et al. 1994) is powered by the SGR, then the quiescent X-ray emission is *not* powered by accretion. (This is in spite [!] of the detection of a highly reddened Be or LBV companion: Kulkarni et al. 1995; Van Kerkwijk et al. 1995.) The luminosity in relativistic particles needed to power the plerion,

$$L_{\mathrm{particle}} \sim 5 \times 10^{36} \left(\frac{D}{8\ \mathrm{kpc}}\right)^{2.5} \left(\frac{t}{10^4\ \mathrm{yr}}\right)^{-1}\ \mathrm{ergs\ s^{-1}}\,, \quad (3)$$

as estimated in Appendix A from the data of Kulkarni et al. (1994) exceeds the quiescent X-ray luminosity (Murakami et al. 1994) by more than 2 orders of magnitude. Thus, the required mass accretion would easily be choked off by the outward ram pressure of the relativistic wind.

Indeed, a few arguments indicate that these relativistic electrons are injected continuously (or at least much more continuously than the SGR bursts themselves). First, the radio emission is peaked within $\lesssim 0''.5$ of the center of SNR G10.0−0.3 (Vasisht et al. 1995), which corresponds to $\sim 1/500$ of the radius of the remnant. The corresponding flow time is less than 1 month at a distance of 8 kpc. Second, the observed burst activity of SGR 1806−20 was concentrated in 1983. If all the particle ejection occurred during bursts, then one would expect to see an even brighter plerion surrounding SGR 0526−66, which emitted a burst containing 100 times the total energy only 4 yr earlier. Third, an SGR burst has such high compactness

$$\ell = \frac{L_\gamma \sigma_T}{m_e c^3 R} \sim 10^7 \left(\frac{L_\gamma}{10^4 L_{\rm edd}}\right)\left(\frac{R}{10\ {\rm km}}\right)^{-1} \quad (4)$$

that nonthermal electrons ejected during the burst would almost instantaneously Compton cool off the photons. And, fourth, the radio flux from SNR G10.0−0.3 is effectively constant on a $\sim 10^7$ s timescale (Vasisht et al. 1995). As noted by Kulkarni et al. (1994), this contrasts with the strong radio flares emitted by accretion-powered sources such as Cir X-1, which also tend to accrete close to the Eddington rate.

The nondetection of a radio plerion surrounding SGR 0526−66 is, in principle, consistent with the enormous energy put out in the March 5 event. The initial 0.15 s hard pulse of that burst appears to have been an expanding fireball (TD95). In a pure electron-positron fireball, the kinetic energy of the pairs is only a minuscule fraction of the total energy after creation/annihilation processes have frozen out. Thus, most of the particle energy is carried by an electron-ion contaminant accompanied by only a small positron component. The radiative signature of the impact of the fireball with the surrounding supernova remnant depends crucially on the coupling between ions and electrons, a piece of physics that is of great interest in external impact models for gamma-ray bursts (Mészáros, Rees, & Papathassiou 1994) and that presently is poorly understood.

3. The X-ray flux from the soft gamma repeaters is some $\sim 10^6$–10^9 times larger in outburst than in quiescence. By contrast, the Rapid Burster brightens only by an order of magnitude when it bursts. This strongly indicates that SGR bursts are not powered by spasmodic accretion from a disk (see also § 7.3 of TD95). Thermonuclear power is also disfavored for SGR 0526−66, since the March 5 event released a million times the energy of a typical Type I X-ray burst. The waiting times between the bursts of SGR 1806−20 have a lognormal distribution (Hurley et al. 1994a), which indicates that the energy source is internal to the star, rather than external impacts that are probably a Poisson process. Indeed, this source shows none of the correlations between fluence and waiting interval characteristic of either Type I or Type II X-ray bursts (Laros et al. 1987).

2.2. *Anomalous X-Ray Pulsars*

The peculiar X-ray pulsar 1E 2259+586 (Gregory & Fahlman 1980) shares a number of properties with SGR 0526−66 (TD93a, TD93b; Corbet et al. 1995). This pulsar has a 7 s spin period and also resides in a $\sim 10^4$ yr old SNR (CTB 109). It has an unusually soft X-ray spectrum with $L_X \simeq (0.5–1) \times 10^{35}$ ergs s^{-1}, a history of continual, nearly steady spin-down (Iwasawa, Koyama, & Halpern 1992), and no detected binary modulation, optical companion, or quiescent radio emission (Coe, Jones, & Lehto 1994, and references therein). Three other X-ray pulsars, 4U 0142+614 (Hellier 1994; Israel, Mereghetti, & Stella 1994), 1E 1048.1−5937 (Seward, Charles, & Smale 1986), and RXJ 1838−03 (Schwentker 1994), also have low luminosities[3] ($L_X \sim 10^{35}$–10^{36} ergs s^{-1}), periods of order 10 s that are steadily increasing, soft spectra, and no detected companions or disks. Together with 1E 2259+586 we refer to these objects as "Anomalous X-ray Pulsars" or AXPs (see DT95; Mereghetti & Stella 1995; Van Paradijs, Taam, & Van den Heuvel 1995). These sources should be considered when making estimates of the birthrate of SGR sources. And, in the future, one might expect to detect SGR burst activity from one or more of these objects!

Mereghetti & Stella (1995) have proposed that the $P = 7.66$ s X-ray pulsar 4U 1626−67 also be included in this class of X-ray pulsars. However, a number of properties clearly identify 4U 1626−67 as an accreting low-mass X-ray binary (Mereghetti & Stella 1995, and references therein): (1) a hard spectrum, with spectral index $\alpha \simeq 0.4$; (2) a period derivative that has changed sign (before 1990, the pulsar was spinning up); (3) quasi-periodic flares with a characteristic timescale of ~ 1000 s; (4) a companion star identified in optical; and (5) optical pulsations that can be attributed to reprocessing of X-ray pulses occurring near the companion star.

The four other X-ray pulsars identified above share essentially none of these properties with 4U 1626−67. Their X-ray spectra are softer than those of verified accreting X-ray binaries (although this possibly is consistent with accretion given their low X-ray luminosities). The spectra can be fitted to power laws with spectral indices in the range of 2.3–4. Planck functions have also given some adequate fits with $T \lesssim 0.8$ keV, as have spectral functions with both blackbody and power-law components (see the fourth row of Table 1). Note that AXPs are observed across substantial distances in the galactic disk, with intervening hydrogen column densities $N_{\rm H} \sim 10^{22}$ cm^{-2}. Thus, their X-rays are heavily absorbed at energies below a few keV, which restricts our knowledge of the intrinsic spectral shapes.

A more direct argument that the AXPs are not low-mass X-ray binaries is based on the association of two of them (1E 2259+586 and RXJ 1838−0301) with SNR of age $\sim 10^4$ yr. (The error box of 1E 1048−593 lies within the Carina nebula, in a zone of vigorous star formation activity.) The association of N such systems with *young* supernova remnants of age $t_{\rm SNR} \sim 10^4$ yr leads to the unsatisfactory conclusion that the Galaxy should contain

[3] In the case of SGR 1806−20, the value of L_X may be biased by the strong low-frequency absorption, corresponding to an electron column density of $\sim 6 \times 10^{22}$ cm^{-2} (Murakami et al. 1994; Sonobe et al. 1994). As a result, the X-ray bolometric flux could contain a significant undetected blackbody component (S. R. Kulkarni, private communication). By contrast, nebular emission may bias *upward* the softer X-ray emission of SGR 0526−66, which is somewhat larger ($L_X \simeq 7 \times 10^{35}$ ergs s^{-1} assuming a blackbody spectrum; Rothschild et al. 1994). In addition, the electron column toward 1E 2259+586 is only $\simeq 6 \times 10^{21}$ cm^{-2} (Corbet et al. 1995), and a two-component power-law and blackbody model is required to give a good fit to the *ASCA* spectrum. The total X-ray luminosity of this anomalous X-ray pulsar is probably not biased significantly by absorption.

$\sim 10^4 (N/3)(t_{SNR}/10^4\ \mathrm{yr})^{-1}(t_{GW}/3 \times 10^7\ \mathrm{yr})$ X-ray pulsars of similar luminosity and spin period. Here $t_{GW} \sim 10^7$–10^8 yr is the timescale on which a binary containing a neutron star and a low-mass Roche lobe–filling stellar companion contracts because of gravity-wave emission (see, e.g., Verbunt 1990). An additional argument against this scenario (considered also by van Paradijs et al. 1995), that the companion star would fall out of contact with its Roche lobe after the formation of the neutron star, is less compelling. If the neutron star received a small kick at formation, then the resulting elliptical orbit would circularize in much less than $\sim 10^4$ yr. The tidal circularization time of the orbit of a fully convective companion is (Zahn 1989)

$$t_{\rm circ} \sim 1\left(\frac{M_2}{M_\odot}\right)^{1/3}\left(\frac{R_2}{R_\odot}\right)^{2/3}\left(\frac{L_2}{L_\odot}\right)^{-2/3}\left(\frac{a}{2R_2}\right)^{8} \mathrm{yr}\,. \quad (5)$$

Depending on the parameters of the orbit, the companion could still be in contact following circularization.

The AXPs have no detected stellar companions down to faint magnitude limits in the optical and infrared (see the seventh row of Table 1). In particular, the upper limit on the optical emission from 1E 2259+586, after accounting for extinction, lies a factor ~ 10 below the level expected from a low-mass X-ray binary of similar X-ray luminosity (Baykal & Swank 1996; cf. Van Paradijs & McClintock 1994). The proper motions of the AXPs are not well enough determined to make reliable inferences about the presence or absence of stellar companions; see Appendix B for a discussion.

The known AXPs have pulse periods in the range of $P = 5$–9 s (see the first row of Table 1) and period derivatives $\dot{P} = 0.5$–15×10^{-12}. Both 1E 2259+586 and 1E 1048−593 have histories of uniform spin-down, tracked over a decade or so.[4] Perhaps the strongest argument in favor of accretion as the energy source for the X-ray emission of 1E 2259+586 is that the inferred accretion rate is just about what is required *if* the neutron star is close to its equilibrium spin period $P_{\rm eq}$, and if it has a dipole field of strength $B \sim 10^{12}$ G, as is typical for a young pulsar (Iwasawa et al. 1992). One may write (see, e.g., Bhattacharya & van den Heuvel 1991)

$$P_{\rm eq} = 10\left(\frac{B_{\rm dipole}}{5 \times 10^{11}\ \mathrm{G}}\right)^{6/7}\left(\frac{L_{\rm X}}{10^{35}\ \mathrm{ergs\ s^{-1}}}\right)^{-3/7} \mathrm{s}\,. \quad (6)$$

However, almost the same scaling between P and $B_{\rm dipole}$ (with quite a different proportionality) is obtained under the assumption that the neutron star is isolated and has spun down by the torque of a relativistic MHD wind. Approximating this torque as magnetic dipole radiation (Pacini 1967) yields

$$P = 8.8\left(\frac{t}{10^4\ \mathrm{yr}}\right)^{1/2}\left(\frac{B_{\rm dipole}}{10^{15}\ \mathrm{G}}\right)\left(\frac{R}{10\ \mathrm{km}}\right)^{2}\left(\frac{M}{1.4\ M_\odot}\right)^{-1/2} \mathrm{s}\,. \quad (7)$$

As we show in § 3, a surface X-ray flux $L_{\rm X} \sim 10^{35}$ ergs s^{-1} would be driven by the decay of such a strong magnetic field. The amplitude of this flux is limited by neutrino emission to be less than $L_{\rm X} \sim 10^{35}$–10^{36} ergs s^{-1} (depending on details such as the superfluid state of the core; see also Van Riper 1991; TD93a). As a result, one has two almost equally natural relations between the observed period and X-ray flux of an X-ray pulsar. The magnetar model should be considered in a situation in which (1) the X-ray spectrum is relatively soft; (2) the source is associated with a young supernova remnant; (3) the source has been spinning down almost continuously, without episodes of sustained spin-up; or (4) the source has emitted soft gamma repeater bursts.

More generally, in the magnetar model, one can estimate the dipole magnetic fields of the AXPs in two ways. One can either ask what field is required to drive the present, measured spin-down rate [$B_{\rm dipole}(P, \dot{P})$, in the tenth row of Table 1], or how strong the field must have been to spin down the star to period P (from a much smaller initial period) in the age of the associated supernova remnant [$B_{\rm dipole}(P, t_{\rm SNR})$, in the eleventh line Table 1]. In both cases the spin-down mechanism is idealized as vacuum magnetic dipole radiation. Note that for 1E 2259+586, the two determinations of $B_{\rm dipole}$ are discrepant by a factor ~ 4. This could indicate a decrease in the dipole field strength during the star's lifetime (perhaps by an interchange instability: Flowers & Ruderman 1977; § 15.2 in Thompson & Duncan 1993b) or a systematic error in the age of the SNR.

A strong bound on the radio intensity of 1E 2259+586, $< 50\mu$Jy at 1.5 GHz with 3 σ confidence, was found by Coe et al. (1994). This is fainter that predicted by empirical pulsar radio luminosity fits when extrapolated into the AXP domain of $\{P, \dot{P}\}$ (cf. § 3.3 of DT92). However, these empirical relations are very uncertain at low luminosity, and the beaming angle of the radio emission is probably quite small (Kulkarni 1992).

Evidence that might favor the interpretation of 1E 2259+586 as an accreting neutron star is the observed variation in $L_{\rm X}$ by a factor 2 between 1989 and 1993 (Iwasawa et al. 1992; Corbet et al. 1995). However, the amplitude and timescale of this variation could also be modeled as a variation of the internal magnetic dissipation rate, with a timescale of ~ 1 yr arising naturally as the thermal conduction time from the base of the neutron star crust to its surface (§ 4.2).

2.3. *A White Dwarf Model*

One other model for 1E 2259+586 should be mentioned. Paczyński (1990) suggested that 1E 2259+586 is an isolated, magnetized white dwarf (see also Morini et al. 1988). A white dwarf, with its larger moment of inertia, yields a much greater spin-down luminosity for a given spin period and period derivative than does a neutron star. In the case of 1E 2259+586, one infers an efficiency of X-ray emissions, $L_{\rm X}/|I\omega\dot{\omega}| \sim 10^{-2}$, where I is the white dwarf moment of inertia. (Of course, the possibility of powering X-rays with the release of magnetic rather than rotational energy provides a loophole to this argument.) Usov (1993) pointed out that spin-down will drive relativistic pair currents in the white dwarf magnetosphere. He suggests that the observed keV energy thermal X-rays are emitted by hot gas that is heated by a back flux of positrons onto the star. But the size of the X-ray-emitting area is

$$R = \left(\frac{L_{\rm X}}{\pi\sigma_{\rm SB}T^4}\right)^{1/2} = 10L_{35}^{1/2}\left(\frac{T}{0.42\ \mathrm{keV}}\right)^{-2} \mathrm{km}\,,$$

[4] A 1.6 σ detection of a brief spin-up phase in 1E 2259+586 (Baykal & Swank 1996) could, if real, be easily explained by a neutron star glitch (§ 4.2; TD93b), or possibly by a glitch in a massive white dwarf with an iron core (Usov 1994).

TABLE 1

ANOMALOUS X-RAY PULSARS (AXPs)

PARAMETER	OBJECT			
	1E 2259+586[a]	1E 1048−593[b]	4U 0142+614[c]	RXJ 1838−0301[d]
P (pulse period) (s)	6.98	6.44	8.69	5.45
$\dot{P}$ (s s^{-1})	5.0×10^{-13}	1.5×10^{-11}	2.3×10^{-12}	Not yet measured
L_X (ergs s^{-1})	$\sim 2 \times 10^{35}\left(\frac{D}{5\ \text{kpc}}\right)^2$	$2\text{–}8 \times 10^{35}\left(\frac{D}{10\ \text{kpc}}\right)^2$	$\sim 10^{36}\left(\frac{D}{4\ \text{kpc}}\right)^2$	$\sim 3 \times 10^{35}\left(\frac{D}{3\ \text{kpc}}\right)^2$
X-Ray Spectrum (published fits)	Best-fit: combination $\alpha \approx 4$ power-law + $T \approx 0.42$ keV blackbody	$\alpha \approx 2.3$ power-law	$\alpha \approx 2.5\text{–}4$ power-law	$\alpha \approx 2.7$ power-law or $T \approx 0.8$ keV Blackbody
N_H [cm^{-2}] inferred from X-ray absorption	1×10^{22}	$\sim 2 \times 10^{22}$	$\sim 1.5 \times 10^{22}$	$\sim 1 \times 10^{22}$
Location	In supernova remnant (SNR) with age $t_{SNR} \sim 1.3 \times 10^4$ yr	40′ E of η Carinae; Behind Carina nebula? No identified SNR	Behind molecular cloud with $N_H \sim 10^{22}$ cm^{-2}; No identified SNR	In SNR with age $t_{SNR} \sim 3 \times 10^4$ yr (roughly estimated)
Bounds on companion Star	$V \gtrsim 23$ (main-sequence K star)	V > 20	$V > 24$, $R > 22.5$	No verified companion
$\Delta\theta$ (displacement from SNR center)	3.′1 to east	...	...	∼20′ to southeast
$V_{trans}(\Delta\theta, t_{SNR})$	$\sim 340\left(\frac{D}{5\ \text{kpc}}\right)$ km s^{-1}	...	...	$\sim 600\left(\frac{D}{3\ \text{kpc}}\right)$ km s^{-1}
$B_{dipole}(P, \dot{P})$ (G)	0.7×10^{14}	4×10^{14}	2×10^{14}	...
$B_{dipole}(P, t_{SNR})$ (G)	3×10^{14}	...	...	2×10^{14}

[a] REFERENCES.—Corbet et al. 1995; Iwasawa et al. 1992; Wang et al. 1992; Coe et al. 1994; Gregory et al. 1983; and references cited therein.
[b] REFERENCES.—Mereghetti et al. 1992; Corbet & Day 1990; Seward et al. 1986; and references cited therein.
[c] REFERENCES.—Hellier 1994; Israel et al. 1994; Stenle et al. 1987; Mereghetti & Stellar 1995; and references cited therein.
[d] REFERENCES.—Schwentker 1994; Mereghetti & Stella 1995; and references cited therein.

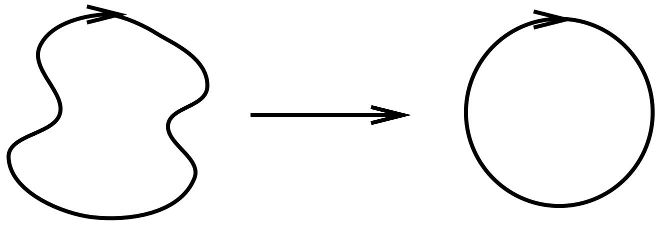

FIG. 1.—A closed loop of magnetic flux lies on an equipotential surface of the neutron star. The lowest energy configuration is a circle.

where $T \approx 0.42$ keV is the best-fit spectral temperature (Corbet et al. 1995). Such a small hot spot is implausible on an $R \sim 3000$ km white dwarf and strongly suggests a neutron star. In addition, it is not obvious why a white dwarf should be the stellar remnant of a supernova explosion. Paczyński (1990) suggests that the surrounding "supernova remnant" may have been a by-product of a white dwarf binary merger, although it is not clear why energy should be released fast enough to produce an expanding shock of energy $\sim 10^{50}$ ergs. Spin-down of a massive white dwarf from an initial period of ~ 2 s would inject this much total energy but would have difficulty reproducing the strong sulfur line emission from the surrounding nebula (Blair & Kirshner 1981). In § 4.2, we briefly discuss spin-down glitches in the white dwarf model.

3. DECAY OF A VERY STRONG MAGNETIC FIELD IN A NEUTRON STAR

If accretion does not power the quiescent X-ray emission of the SGR sources, what does? The identification of SGR 0526−66 with a $B_{\rm dipole} \simeq 6 \times 10^{14}$ G neutron star (DT92; Paczýnski 1992; TD95) introduces a new source of free energy besides rotation and accretion: the magnetic field itself. We now show that energy deposition by the decaying field will power quiescent X-ray emission from the surface and, if the crustal magnetic field lies within a certain range, a steady stream of low-amplitude Alfvén waves in the magnetosphere.

3.1. *Stability Considerations*

It is straightforward to find magnetostatic equilibria of a gravitationally bound fluid star, but the stability of these equilibria is not yet fully understood from first principles. Nonetheless, the existence of white dwarf stars with external magnetic fields as strong as $\sim 5 \times 10^8$ G (see, e.g., Schmidt & Smith 1995) provides an empirical demonstration that stable equilibria do exist in the absence of any rigidity, such as is associated with neutron star crusts. Thus, while a magnetic field stronger than $\sim 10^{14}$ G is capable of stressing the crust to the point that it fractures, magnetostatic equilibria with stronger fields are possible in principle and can in practice be generated by a turbulent dynamo operating in a newborn neutron star (TD93a).

The unstable modes of the magnetic field are severely limited if the star is stably stratified (as is the interior of a neutron star; Reisenegger & Goldreich 1992). A *purely* poloidal magnetic field is unstable to deformations that increase the multipole order of the external field (Flowers & Ruderman 1977) while leaving the internal magnetic energy unchanged. This rearrangement of magnetic field lines can be achieved entirely by displacements along equipotential surfaces. A purely toroidal magnetic field is also unstable to a kink mode (Tayler 1973), but this instability is confined to a small distance

$$\frac{\varpi}{R_\star} \sim \frac{R_\star}{\sqrt{4\pi P}} \frac{\partial B_\phi}{\partial \varpi} (\varpi = 0) \tag{8}$$

from the axis of symmetry.

The stability of more complicated field configurations can be analyzed under the assumption that the magnetic field is confined to slender flux ropes. Consider, for example, a closed loop of magnetic flux that lies within a radial shell[5] of thickness δR (Fig. 1). In a convectively stable region, the loop is supported against collapse by the pressure of the enclosed material, since this material can flow only along an equipotential surface. That is, each loop can be labeled by a conserved quantity, the enclosed solid angle $\delta\Omega$ [or, equivalently, the enclosed mass $\delta M = \rho(R) R^2 \, \delta\Omega \, \delta R$]. The magnetic energy is minimized when the circumference of the loop is minimized, that is, when the loop is a circle.

This configuration is easily generalized to one in which each radial shell contains several loops, with the radial component of $\boldsymbol{B}$ still being assumed to vanish. The magnetic flux of each loop has two possible orientations. Loops with the same orientation are able to merge by reconnecting (Fig. 2), but separate loops with opposite orientations cannot merge. (Conversely, if one loop is contained by the second loop, then the selection rules are reversed: only loops with opposing orientations can merge; Fig. 3)

Each merger conserves the enclosed mass and reduces the magnetic energy by reducing the total length of the bounding magnetic flux tube. It is straightforward to see that the

[5] We neglect the backreaction of the magnetic field on the stellar density profile, as well as the effects of rotation in what follows.

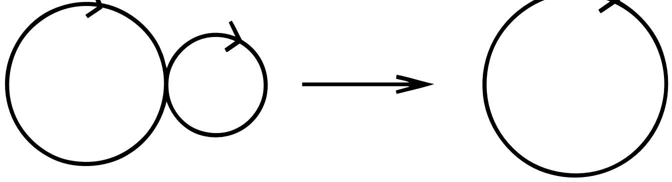

FIG. 2*a*

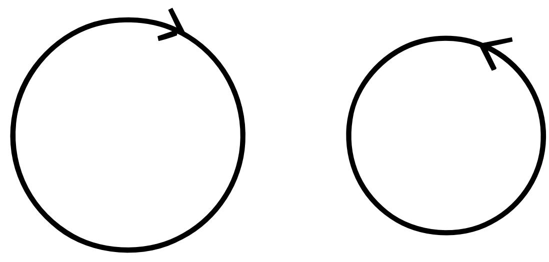

FIG. 2*b*

FIG. 2.—(*a*) Two loops with the same orientation merge by reconnecting, thereby reducing their total length while conserving the total mass enclosed by the loops. (*b*) Two separate loops with opposite orientations cannot merge. It is energetically favored for all loops with the same orientation to merge together into one loop.

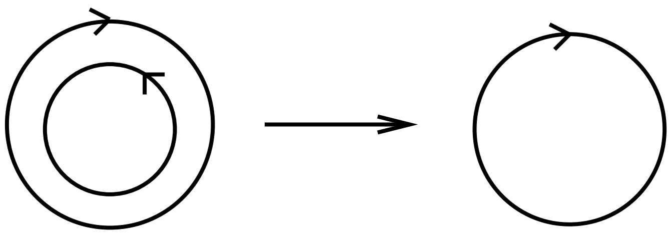

FIG. 3.—When one loop of magnetic flux is contained by a second loop, the merger rules are reversed.

minimum energy configuration is one in which all loops of a given orientation within each radial shell have merged into a single loop (Fig. 2*b*). Since the mass enclosed by all loops of a given orientation is always less than the total mass of the shell, one deduces that the circumference of the single merged loop is always less than $2\pi R$ (Fig. 3).

The main conclusion to draw from this analysis is that stable magnetostatic equilibria with $B_\phi \gg B_P$ certainly do exist. A helical dynamo operating in a newborn neutron star probably generates a toroidal magnetic field that is much stronger than the external dipole component.[6] A finite value of $\partial B_\phi/\partial\varpi(\varpi = 0)$ corresponds to a finite current density at the symmetry (rotation) axis, and so the abovementioned kink instability merely forces this current away from the axis (Tayler 1973).

How then can an initially stable field configuration become unstable? The magnetic field diffuses through the interior of a neutron star on a timescale that is calculated in § 3.3. As a result, toroidal and poloidal field components are interchanged. Whether diffusion on a long timescale can lead to a *sudden* hydromagnetic instability [with a growth time $\sim R_\bigstar/V_{\rm A}$, where $V_{\rm A} \sim B/(4\pi\rho)^{1/2}$], we do not have a clear answer. The rigid crust will stabilize the internal magnetic field as long as the Maxwell stresses applied to it have magnitude $B_{\rm frac}^2 \lesssim \theta_{\max}\mu$ (where μ is the shear modulus and $\theta_{\max} \sim 10^{-4}$ to 10^{-2} is the yield strain). If B is stronger than $B_{\rm frac}^2/4\pi$, then the growth time of the instability is $\sim 0.1(\Delta\ell/1\ {\rm km})(B/B_{\rm frac})^{-1}$ s, where $\Delta\ell$ is the nonradial displacement of the magnetic field lines and μ is the shear modulus. This timescale is comparable to the ~ 0.15 s duration of the initial hard transient phase of the 1979 March 5 burst (TD95). Larger displacements would release more energy than was radiated during the March 5 burst if the dipole magnetic field is $\sim 6 \times 10^{14}$ G (as several arguments indicate for SGR 0526−66; § 2.).

3.2. *Ambipolar Diffusion in a Stratified Medium*

The electrical conductivity in the core of a neutron star is so large (Baym et al. 1969) that the magnetic field is effectively tied to the charged particle component (the electrons and protons). As a result, the magnetic field drags the charged particles with it as it diffuses through the core. The rate of ambipolar diffusion maybe limited predominantly *either* by collisions between protons and the neutral component (the neutrons) *or* by pressure gradient forces (Goldreich & Reisenegger 1992, hereafter GR92). (These separate regimes have been considered by Shalybkov & Urpin 1995 and by Pethick 1992.)

The drift velocity $\boldsymbol{v}_e$ of the electrons can be separated into two components: one associated with the current needed to support the magnetic field, and another associated with the collective ambipolar drift of the electrons and protons through the neutron fluid,

$$\boldsymbol{v}_e = \boldsymbol{v}_p + \frac{\boldsymbol{j}}{n_e e} = \boldsymbol{v} + \frac{\boldsymbol{j}}{n_e e} . \tag{9}$$

We demonstrate in the next section that $v \gg j/n_e e$ for the values of B and T appropriate to the core of a young magnetar. In this regime, the relation between the ambipolar drift velocity $\boldsymbol{v}$ and the Lorentz force $\boldsymbol{j} \times \boldsymbol{B}$ can be written (GR92)

$$\frac{m_p}{\tau_{pn}}\,\boldsymbol{v} + \nabla(\mu_p + \mu_e - \mu_n) = \frac{\boldsymbol{j} \times \boldsymbol{B}}{n_e} . \tag{10}$$

The first term on the left-hand side represents proton-neutron drag, with $\tau_{pn} = 3.3 \times 10^{-17} T_8^{-2} \rho_{15}^{1/3}$ s corresponding collision time[7] in a normal *n-p-e* degenerate plasma (Yakovlev & Shalybkov 1990). The second term represents pressure gradient forces which oppose the Lorentz force. When this term dominates, the diffusion rate is limited by the rate at which the charged particle species relax back to β-equilibrium. The divergence of the flux of electrons and protons differs from zero only to the extent that the beta reactions $p + e^- \to n + \nu_e$ and $n \to p + e^- + \bar{\nu}_e$ are allowed,

$$\nabla \cdot (n_e \boldsymbol{v}) = -\lambda(\mu_p + \mu_e - \mu_n) . \tag{11}$$

Modified URCA reactions yield a rate constant $\lambda = 1.1 \times 10^{28} T_8^6 \rho_{15}^{2/3}$ ergs^{-1} cm^{-3} s^{-1} (Sawyer 1989). Equation (10) then becomes

$$\frac{m_p}{\tau_{pn}}\,\boldsymbol{v} - \frac{1}{\lambda}\,\nabla(\nabla \cdot n_e \boldsymbol{v}) = \frac{\boldsymbol{j} \times \boldsymbol{B}}{n_e} . \tag{12}$$

Implicit in relation (10) is the fact that a spherically symmetric star can simultaneously be in *exact* chemical and hydrostatic equilibrium at zero temperature. By exact hydrostatic equilibrium, we mean that each particle species is separately in hydrostatic equilibrium, so that the net frictional force between each pair of species vanishes. Let us suppose that the star is composed of N species of fermions which can undergo the reaction

$$f_1 + f_2 + \cdots + f_j = f_{j+1} + \cdots + f_N . \tag{13}$$

The corresponding condition of chemical equilibrium is

$$\mu_1 + \mu_2 + \cdots + \mu_j = \mu_{j+1} + \cdots + \mu_N . \tag{14}$$

The general relativistic equation of hydrostatic equilibrium for particle species $1 \le i \le N$ reads (see, e.g., Shapiro & Teukolsky 1983)

$$-\nabla P_i = (P_i + \rho_i)\nabla\Phi , \tag{15}$$

or equivalently

$$-\nabla\mu_i = \mu_i \nabla\Phi , \tag{16}$$

[6] This is true of the solar dynamo. Even if the toroidal field concentrated in the shear layer at the base of the convection zone were spread out in radius, B_ϕ would still exceed the external dipole field by 2 orders of magnitude. An important distinction between a magnetar and the Sun is that the density scale height at the top of the convection zone that forms during the first ~ 30 s of neutrino cooling is a relatively large fraction ~ 0.03 of the stellar radius. This suggests that $B_{\rm dipole}/B_\phi$ is larger in the neutron star than it is in the Sun.

[7] We normalize the mass density to $\rho = \rho_{15} \times 10^{15}$ g cm^{-3} and the temperature to $T = T_8 \times 10^8$ K.

where we make use of the thermodynamic relations $\nabla P_i = n_i \nabla \mu_i$ and $P_i + \rho_i = n_i \mu_i$ between the pressure, energy density ρ_i, particle density n_i, and chemical potential μ_i. One sees that equations (14) and (16) are consistent upon the appropriate summation of (16) over particle species. The conclusion would be different if the right-hand side of equation (15) depended on something other than the enthalpy density $P_i + \rho_i$.

At very high temperatures, β-equilibrium is established rapidly, the drag term in equation (12) dominates and

$$\frac{m_p}{\tau_{pn}} \boldsymbol{v} \simeq \frac{1}{n_e} \boldsymbol{j} \times \boldsymbol{B} \quad (T \gg T_{\rm trans}) . \tag{17}$$

The transition to the regime in which the pressure gradient and gravitational forces dominate occurs at a temperature $T_{\rm trans}$, which is given by

$$\frac{\lambda m_n L^2}{n_e \tau_{pn}} = \left(\frac{T}{T_{\rm trans}}\right)^8 = 1 . \tag{18}$$

Here L is the gradient scale of the magnetic field. In a normal *n-p-e* plasma, this works out to be

$$T_{\rm trans} = 6.9 \times 10^8 \rho_{15}^{1/12} \left(\frac{L_6}{0.2}\right)^{-1/4} \left(\frac{Y_e}{0.05}\right)^{1/8} \text{ K} , \tag{19}$$

where Y_e is the electron fraction, $L = L_6 \times 10^6$ cm, and $L \simeq 3$ km is the depth in a 10 km radius neutron star that encompasses half the mass.

If the critical temperature $T_{\rm cr}$ for $^3P_2$ neutron pairing exceeds $T_{\rm trans}$, then ambipolar diffusion becomes limited by pressure gradient forces at the higher temperature $\sim T_{\rm cr}$ (see § 3.8.).

The equation of hydrostatic equilibrium

$$-\nabla P + \boldsymbol{j} \times \boldsymbol{B} + (\rho + P)\boldsymbol{g} = 0 \tag{20}$$

provides additional constraints on the velocity field. One sees that $\nabla \times (\boldsymbol{j} \times \boldsymbol{B}) = 0$ as long as the density perturbation can be neglected in the force balance (the Cowling limit). This suggests that at high temperatures ($T > T_{\rm trans}$), where the charged particle flux $n_e \boldsymbol{v}$ and $\boldsymbol{j} \times \boldsymbol{B}$ are proportional, that $n_e \boldsymbol{v}$ is approximately irrotational.

Goldreich & Reisenegger (1992) have noted that the charged particle flux may be separated into a solenoidal mode $[\nabla \cdot (n_e \boldsymbol{v}) = 0]$ that does not perturb chemical equilibrium and an irrotational mode $[\nabla \times (n_e \boldsymbol{v}) = 0]$ that does. At high temperatures, the two modes are degenerate, but at low temperatures ($T < T_{\rm trans}$), the solenoidal mode has a much faster growth rate, since it is does not engender an opposing pressure gradient force. Urpin & Ray (1994) and Shalybkov & Urpin (1995) have treated ambipolar diffusion in the core of a neutron star without explicitly taking into account the effect of pressure gradient forces or the distinction between these two modes.

Is the solenoidal mode excited? At this point, it is important to note that the magnetic field and the entrained fluid is in magnetostatic equilibrium. Solenoidal perturbations of such a field configuration that reduce the magnetic energy are very limited. Consider first a magnetic flux rope immersed in a uniform *n-p-e* plasma without a gravitational field (Fig. 4). The flux rope then relaxes to magnetostatic equilibrium on the Alfvén timescale $L/V_{\rm A}$, which is much shorter than the growth time $t^s_{\rm amb} = 4\pi L^2 n_e m_p / B^2 \tau_{pn}$ of the solenoidal mode of ambipolar diffusion. As a result, the

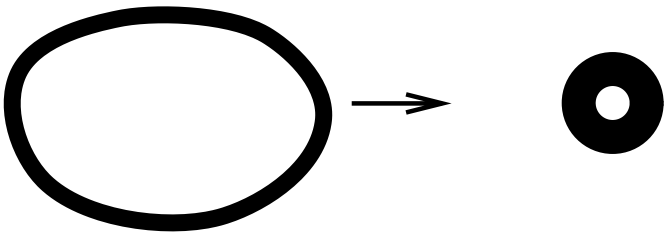

FIG. 4.—A loop of magnetic flux immersed in a homogeneous *n-p-e* plasma relaxes to magnetostatic equilibrium. Magnetic tension drives the loop to contract to a compact toroidal configuration with an O-type neutral point. In the limit that the magnetic pressure is much less than the gas pressure, the volume of the flux loop is constant.

neutrons and the charged particles share the same velocity field $\boldsymbol{v}_{\rm hydro}$. This velocity field is approximately solenoidal when $B^2/8\pi P \ll 1$, and the fractional density deficit inside the flux tube is small.

Now consider how the flux rope evolves on a timescale $t^s_{\rm amb}$. The hydromagnetic motion of the plasma will induce departures from β-equilibrium of order $(B^2/8\pi P)Y_e$, but the initial temperature is assumed high enough that the plasma relaxes back to β-equilibrium on a timescale short compared to $t^s_{\rm amb}$. It is also assumed that the plasma cools down enough that the β-reactions are frozen on a timescale $t^s_{\rm amb}$.[8] Then the charged particles are tied to the magnetic field lines, and their velocity field $\boldsymbol{v}_{\rm amb}$ satisfies the same constraint as did $\boldsymbol{v}_{\rm hydro}$, namely

$$\nabla \cdot \boldsymbol{v}_{\rm amb} = \nabla \cdot \boldsymbol{v}_{\rm hydro} = 0 . \tag{21}$$

Since the flux rope, after achieving magnetostatic equilibrium, was stable to all solenoidal hydrodynamical displacements, it is likewise stable to all solenoidal displacements by ambipolar diffusion.

This simple argument no longer holds when the *n-p-e* plasma is stably stratified. During relaxation to magnetostatic equilibrium, fluid parcels are forced to move along equipotential surfaces, and the velocity $\boldsymbol{v}_{\rm hydro}$ is subject to the dual constraint

$$\nabla \cdot (\rho \boldsymbol{v}_{\rm hydro}) = 0; \quad \boldsymbol{v}_{{\rm hydro},z} = 0 . \tag{22}$$

This allows complicated equilibria that would undergo further relaxation if motions in all three dimensions were allowed (TD93b). For example, reconnection at a discontinuity in $\boldsymbol{B}$ is forbidden if the vertical component of the field on opposite sides of the discontinuity has opposite signs. Nonetheless, *vertical diffusive motions of the electrons and protons across the neutrons are still allowed*, and so $\boldsymbol{v}_{\rm amb}$ is subject only to the weaker constraint $\nabla \cdot (\rho \boldsymbol{v}_{\rm amb}) = 0$. Figure 5*a* gives the example of two neighboring flux ropes, along which the flux density varies in the vertical direction. Correlated diffusive motions of the electrons and protons along the two loops, which conserve the total number of charged particles on each equipotential surface, will reduce the total magnetic energy (Fig. 5*b*). Nonetheless, a much larger fraction of the magnetic energy can be tapped by the irrotational mode, which causes the flux ropes to spread out laterally and to rise in the vertical direction.

[8] These conditions are appropriate to a cooling neutron star in which the convective motions that amplify the magnetic field turnoff at an age of ~ 30 s, when the temperature is ~ 1 MeV (TD93a). Of course, the decomposition into solenoidal and irrotational modes is meaningful only if the β-reactions are frozen on a timescale $t^s_{\rm amb}$, that is, if $T < T_{\rm trans}$.

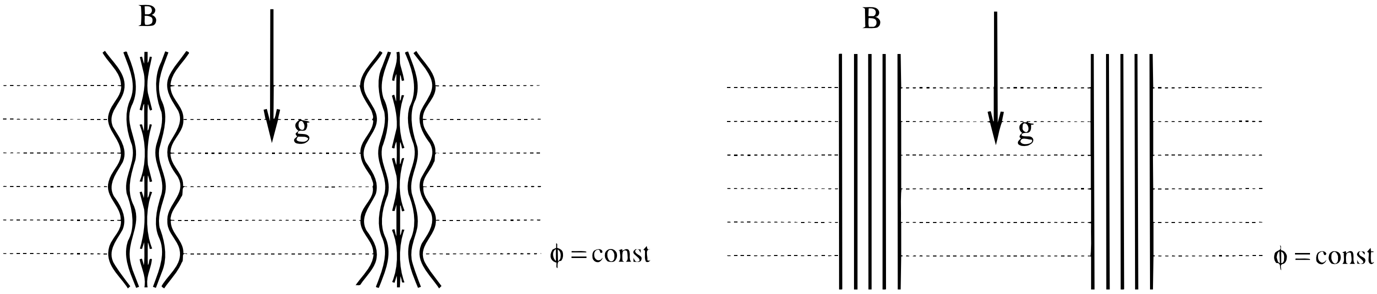

FIG. 5*a* FIG. 5*b*

FIG. 5.—Two neighboring magnetic flux ropes are immersed in a *n-p-e* plasma in a gravitational field. Irregularities in the flux density on the two ropes (*a*) can be smoothed out by the solenoidal mode of ambipolar diffusion in a correlated manner, reaching the configuration of (*b*). However, most of the magnetic energy is tapped only by diffusive motions that have nonvanishing divergence.

These physical arguments can be quantified by considering a harmonic perturbation $\delta \boldsymbol{B}(x) = \delta \boldsymbol{B}_0\, e^{i\boldsymbol{k}\cdot\boldsymbol{x}}$ of a uniform background magnetic field $\boldsymbol{B}_0$. We separate the ambipolar diffusion velocity (which is also harmonic with the same wavevector) into components $\boldsymbol{v}_{\rm amb}^{\perp}$ and $\boldsymbol{v}_{\rm amb}^{\parallel}$ perpendicular and parallel to $\boldsymbol{k}$. These components represent the solenoidal and irrotational modes of ambipolar diffusion.

In Fourier variables, equation (12) becomes

$$\left(\frac{m_p}{\tau_{pn}}\right)\boldsymbol{v}_{\rm amb} - i\left(\frac{k n_e v_{\rm amb}^{\parallel}}{\lambda}\right)\boldsymbol{k} = -\frac{i}{n_e}\left[(\boldsymbol{k}\cdot\boldsymbol{B}_0)\delta\boldsymbol{B} - (\delta\boldsymbol{B}\cdot\boldsymbol{B}_0)\boldsymbol{k}\right] \tag{23}$$

to lowest order in $\delta\boldsymbol{B}$. Magnetic flux conservation implies $\boldsymbol{k}\cdot\delta\boldsymbol{B} = 0$, and so the perpendicular component of $\boldsymbol{v}_{\rm amb} = \boldsymbol{v}_{\rm amb\,0}\, e^{i\boldsymbol{k}\cdot\boldsymbol{x}}$ is

$$\frac{m_p}{\tau_{pn}}\, \boldsymbol{v}_{\rm amb\,0}^{\perp} = -i\,\frac{(\boldsymbol{k}\cdot\boldsymbol{B}_0)}{n_e}\,\delta\boldsymbol{B}_0\,. \tag{24}$$

That is, the solenoidal mode of ambipolar diffusion is directed parallel to $\delta\boldsymbol{B}_0$, but $\pi/2$ out of phase. The field configuration shown in Figure 5*a* can be represented most simply by a uniform vertical background field $\boldsymbol{B}_0$, with $\delta\boldsymbol{B}_0$ directed almost parallel to $\boldsymbol{B}_0$ and $\boldsymbol{k}$ directed almost perpendicular to $\boldsymbol{B}_0$ (so that the sign of $\delta\boldsymbol{B}$ varies on a horizontal length scale that is small compared to the vertical wavelength). The case of uniform flux ropes (in which the flux density varies with horizontal position but is independent of *z*) corresponds to the limit $\boldsymbol{k}\cdot\boldsymbol{B}_0 = 0$, which yields $\boldsymbol{v}_{\rm amb\,0}^{\perp} = 0$. In this case, magnetic flux is transported in the horizontal direction at a velocity

$$v_{\rm amb\,0}^{\parallel} = -\frac{(\delta\boldsymbol{B}_0\cdot\boldsymbol{B}_0)\lambda}{n_e^2}\,k \tag{25}$$

where we make use of the inequality $m_p/\tau_{pn} \ll k^2 n_e/\lambda$. This is nothing other than the irrotational mode of ambipolar diffusion.

Now consider the solenoidal mode in a stably stratified medium. Since the fluid is always very nearly in magnetostatic equilibrium,[9] bulk motions of the combined *n-p-e* fluid will act in place of ambipolar diffusion along equipotential surfaces. For example, these bulk motions will erase any solenoidal ($\nabla\cdot\xi = 0$) distortion for which $\delta\boldsymbol{B}_0$ runs parallel to these surfaces, on a timescale much shorter than $t_{\rm amb}^{s}$. But such distortions are very limited, and more general incompressible distortions of the fluid can be erased only on a timescale $t_{\rm amb}^{s}$.

A further complication is that the interior of a neutron star can undergo a hydromagnetic instability long after the β-reactions have frozen out. This implies small departures from β-equilibrium (of order $B^2/8\pi P$) will be generated during the relaxation to magnetostatic equilibrium.

We conclude that the solenoidal mode of ambipolar diffusion is capable of smoothing out inhomogeneities *along* flux ropes in the core of a neutron star but that large-scale reorganizations of the field probably are inhibited by pressure gradient forces. This suggests that the solenoidal mode of ambipolar diffusion makes only a modest contribution to the total dissipation rate of magnetic field energy. The assumption that ambipolar diffusion is limited only by the drag force (as made by Urpin & Ray 1994 and Shalybkov & Urpin 1995) leads in general to an overestimate of the magnetic decay rate in the core when $T < T_{\rm trans}$.

3.3. *Heating of the Core by Ambipolar Diffusion*

Ambipolar diffusion of a magnetic field through a stratified medium was critically examined in the previous section. We argued that, since the interior of the star is in magnetostatic equilibrium, solenoidal distortions of the magnetic field $[\nabla\cdot(n_e\,\xi) = 0]$ are limited, and the solenoidal mode of ambipolar diffusion $[\nabla\cdot(n_e\boldsymbol{v}) = 0]$ will release only a fraction of total magnetic energy. The timescale of this mode is very short when the neutrons are superfluid (GR92). The remaining irrotational mode $[\nabla\times(n_e\boldsymbol{v}) = 0]$ can release a large fraction of the magnetic energy (both through friction and through β-reactions) on a longer timescale. In this subsection, we calculate the equilibrium temperature at which the magnetic heating of the core of the neutron star is balanced by neutrino cooling and show that this an interesting source of free energy at an age of $\sim 10^4$ yr. A preliminary account of this effect was given in TD93b.

At low temperatures $T < T_{\rm trans}$, where the diffusion rate is limited mainly by the pressure gradient force rather than by proton-neutron drag, a significant fraction of the field energy is converted to heat. For example, the chemical potential imbalance $\Delta\mu \equiv \mu_p + \mu_e - \mu_n$ is relieved by the modified URCA reactions

$$n + n \rightarrow n + p + e^- + \bar{\nu}_e \tag{26}$$

when $\Delta\mu < 0$, or

$$n + p + e^- \rightarrow n + n + \nu_e\,, \tag{27}$$

[9] Except for motions on the very short Alfvén crossing time.

when $\Delta\mu > 0$. All the particles in the final state share the degeneracy energy that has been released, but only the antineutrino (neutrino) escapes directly. As a result, the heating rate can be estimated as

$$\dot{U}^{+}_{\rm amb} = \frac{B^2}{4\pi t_{\rm amb}}\,, \tag{28}$$

where the timescale of the irrotational mode of ambipolar diffusion (GR92; Pethick 1992)

$$t^{irr}_{\rm amb} = \frac{B}{v\,|\nabla \times \boldsymbol{B}|} \sim \frac{4\pi n_e^2}{\lambda B^2} \quad (T < T_{\rm trans}) \tag{29}$$

can be read directly off equation (12).

When the magnetic field is sufficiently strong, the magnetic energy density is larger than the thermal energy density, and there is a balance between neutrino cooling and magnetic heating. Equating equation (28) with the modified URCA cooling rate (Friman & Maxwell 1979)

$$\dot{U}^{-}_{\rm URCA} = 4 \times 10^{13}\left(\frac{m_n^*}{m_n}\right)^3\left(\frac{m_p^*}{m_p}\right)\rho_{15}^{2/3}T_8^8 \text{ ergs cm}^{-3}\text{ s}^{-1}\,, \tag{30}$$

yields the equilibrium relation between T and B,

$$T_8 = 2.4\left(\frac{B}{10^2 B_{\rm QED}}\right)^2\left(\frac{\rho_{15}}{0.7}\right)^{-1}\left(\frac{Y_e}{0.05}\right)^{-1}\,. \tag{31}$$

In this equilibrium state, the temperature is comparable to the magnitude of the chemical potential offset,

$$T \sim |\Delta\mu|\,. \tag{32}$$

The corresponding ambipolar diffusion time (eq. [29]) is a very strong function of magnetic field strength, density, and electron fraction,

$$t_{\rm amb}(B) = 5 \times 10^6\left(\frac{\rho_{15}}{0.7}\right)^{22/3}\left(\frac{B}{10^2 B_{\rm QED}}\right)^{-14}\left(\frac{Y_e}{0.05}\right)^8 \text{ yr}\,. \tag{33}$$

(We have chosen $m_n^*/m_n = m_p^*/m_p = 0.7$ for the effective mass of the proton and neutron in nuclear matter.) The existence of a balance between heating and cooling allows one to integrate the time evolution equation $dB/dt = -B/t_{\rm amb}$, obtaining

$$B(t) = B_0\left\{1 + 14\left[\frac{t}{t_{\rm amb}(B_0)}\right]\right\}^{-1/14}\,. \tag{34}$$

This equation goes over asymptotically to

$$B(t) = 5.7 \times 10^{15}\left(\frac{t}{10^4\text{ yr}}\right)^{-1/14}\left(\frac{\rho_{15}}{0.7}\right)^{11/21}\left(\frac{Y_e}{0.05}\right)^{4/7}\text{ G}\,. \tag{35}$$

at $t \gtrsim 1/14 t_{\rm amb}(B_0)$. The corresponding core temperature is

$$T_8(t) = 4.1\left(\frac{t}{10^4\text{ yr}}\right)^{-1/7}\left(\frac{\rho_{15}}{0.7}\right)^{1/21}\left(\frac{Y_e}{0.05}\right)^{1/7}\,, \tag{36}$$

and the total neutrino luminosity is

$$L_\nu(t) = 4 \times 10^{36}\left(\frac{t}{10^4\text{ yr}}\right)^{-8/7} \times \left(\frac{\rho_{15}}{0.7}\right)^{22/21}\left(\frac{Y_e}{0.05}\right)^{8/7}\text{ ergs s}^{-1}\,. \tag{37}$$

The $B(t)$ relation (eq. [34]) yields only an 18% reduction in B at $t = t_{\rm amb}$ and a factor of 2 reduction only at $t = 10^3 t_{\rm amb}$. A slightly higher temperature is obtained if B drops significantly on a timescale $t_{\rm amb}$,

$$\frac{\partial}{\partial t}\left(\frac{B^2}{8\pi}\right) = -\frac{B^2}{4\pi t_{\rm amb}} \simeq -\frac{B^2}{8\pi t}\,. \tag{38}$$

A fast initial decay such as this is plausible if the magnetic field releases energy through a *combination* of diffusion and hydromagnetic instabilities. The size of the chemical potential imbalance caused by a large-amplitude hydromagnetic instability is comparable to the one induced by the slower diffusive motion, $|\Delta\mu|/T \sim B^2/8\pi n_e T \simeq 1$. From equation (38), one gets $t_{\rm amb} \simeq 2t$. Then B is larger by a factor $7^{1/14} \simeq 1.15$, T is larger by a factor $\sim 7^{1/7} = 1.3$,

$$T_8(t) = 5.4\left(\frac{t}{10^4\text{ yr}}\right)^{-1/7}\left(\frac{\rho_{15}}{0.7}\right)^{1/21}\left(\frac{Y_e}{0.05}\right)^{1/7} \quad (t_{\rm amb} = 2t)\,, \tag{39}$$

and L_ν is larger by a factor ~ 7 than the analytic solution (eq. [34]) for $B(t)$ would imply.

Relations (31)–(35) become valid only after the magnetar has cooled down below the temperature (eq. [36]) but before the cooling rate of the core becomes dominated by conduction to the surface (§ 3.5.) or conduction into an inner core containing a kaon condensate. The magnetic field channels the heat flow in such a way that (depending on the connectivity of the field) a large fraction of the volume of the core can avoid either form of cooling up to an age of $\sim 10^4$ yr (§ 3.7).

Now let us check under what circumstances the available magnetic energy dominates the thermal energy of the degenerate nuclear matter. In a normal *n-p-e* plasma, the specific heat of the electrons can be neglected to a first approximation, and

$$U_{\rm th} \simeq \frac{1}{2}(C_{V,n} + C_{V,p})T = \frac{1}{2}\left(\frac{\pi}{3}\right)^{2/3}[(1 - Y_e)^{1/3} + Y_e^{1/3}]\left(\frac{\rho}{m_n}\right)^{1/3} m_n^* T^2\,. \tag{40}$$

Substituting $Y_e = 0.05$ in equation (40) and making use of the relation (eq. [31]) between T and B, one finds

$$\frac{B^2/8\pi}{U_{\rm th}} \simeq 90\left(\frac{B}{10^2 B_{\rm QED}}\right)^{-2}\left(\frac{\rho_{15}}{0.7}\right)^{5/3}\left(\frac{Y_e}{0.05}\right)^2\,. \tag{41}$$

The specific heat is greatly reduced if both the neutrons and protons are superfluid. Nonetheless, proton superfluidity is probably quenched in a large part of the core when the rms magnetic field is as large as $B \sim 6 \times 10^{15}$ G. If the neutrons remain superfluid, then $U_{\rm th}$ is reduced below equation (40) only by the modest factor $Y_e^{1/3}[(1 - Y_e)^{1/3} + Y_e^{1/3}]^{-1}$.

Note also that even when ambipolar diffusion in the core is dominated by the solenoidal mode, the resulting temperature is hardly different for $B \sim 10^2 B_{\rm QED}$. Balancing modified-URCA cooling against frictional heating by the solenoidal mode in a normal *n-p-e* plasma, one deduces

$$T_8 = 4.8\left(\frac{B}{10^2 B_{\rm QED}}\right)^{2/5}\left(\frac{\rho_{15}}{0.7}\right)^{-2/15}\left(\frac{Y_e}{0.05}\right)^{-1/10}\left(\frac{L_6}{0.2}\right)^{-1/5}\,, \tag{42}$$

instead of equation (31). (Here, L is the gradient scale of the magnetic field.) The onset of neutron superfluidity would increase the *p-n* collision time (GR92) and therefore allow a fraction of the magnetic energy to be dissipated at earlier times. However, we show in § 3.3 that the decay of the core magnetic field begins to dominate the secular cooling rate only when the magnetar is older than $\sim 10^3$ yr. This suggests that dissipation of a fraction of the magnetic energy at a much younger age, while the core is still hotter than $\sim 10^9$ K, would not significantly increase the surface X-ray flux.

Finally, we note that since $\nabla \cdot \boldsymbol{j} \simeq 0$, the component of the electron drift velocity associated with the current mixes together with the solenoidal mode of ambipolar diffusion, but not with the irrotational mode. Nonetheless, we can check that $v \gg j/n_e e$ for the parameters of interest,

$$\frac{v}{j/n_e e} \sim \frac{B\lambda L^2 e}{n_e c}$$
$$= 1.0 \times 10^2 \left(\frac{t}{10^4 \text{ yr}}\right)^{-13/14} \left(\frac{\rho_{15}}{0.7}\right)^{10/21} \left(\frac{Y_e}{0.05}\right)^{3/7} \left(\frac{L_6}{0.3}\right)^2 . \tag{43}$$

3.4. *Hall Fracturing in the Crust*

When a current flows through a magnetized plasma, an electric field $\boldsymbol{E} = (n_e ec)^{-1}\boldsymbol{j} \times \boldsymbol{B}$ is induced perpendicular to both $\boldsymbol{j}$ and $\boldsymbol{B}$. The resulting Hall drift of the electrons introduces a term

$$\left(\frac{\partial \boldsymbol{B}}{\partial t}\right)_{\text{Hall}} = -\nabla \times \left(\frac{\boldsymbol{j} \times \boldsymbol{B}}{n_e e}\right) \tag{44}$$

in the induction equation. The effects of Hall drift on transport of magnetic fields in the crust of a neutron star have been considered by Jones (1988) and GR92.

The Hall effect is nondissipative. It will not cause a magnetic flux tube to spread in the direction perpendicular to the axis of the tube. Nonetheless, there do exist wavelike excitations with a component of $\boldsymbol{k}$ parallel to the background magnetic field. Substituting $\boldsymbol{B} = \boldsymbol{B}_0 + \delta\boldsymbol{B} = \boldsymbol{B}_0 + \delta\boldsymbol{B}_0 e^{i\boldsymbol{k}\cdot\boldsymbol{r}}$ into equation (44), one obtains

$$\frac{\partial \delta\boldsymbol{B}}{\partial t} = \left(\frac{cB_0 k_\parallel}{4\pi n_e e}\right)\boldsymbol{k} \times \delta\boldsymbol{B} \tag{45}$$

to lowest order in $\delta\boldsymbol{B}$. Here $k_\parallel$ is the component of $\boldsymbol{k}$ parallel to $\boldsymbol{B}_0$. Since $\boldsymbol{k} \cdot \delta\boldsymbol{B} = 0$ (from the equation of flux conservation), one sees that the polarization vector of the wave rotates at the basic angular frequency of the wave, which is

$$\omega = \frac{ck|\boldsymbol{k} \cdot \boldsymbol{B}|}{4\pi n_e e} \tag{46}$$

(Kingsep, Chukbar, & Yan'kov 1990; GR92).

The corresponding transport time ω^{-1} across a scale length $L = k^{-1}$ is

$$t_{\text{Hall}}(B, L) \sim 1 \times 10^7 B_{15}^{-1} \left(\frac{L_6}{0.3}\right)^2 \left(\frac{\rho_{15}}{0.7}\right)\left(\frac{Y_e}{0.05}\right) \text{ yr} . \tag{47}$$

Even when the core magnetic field is as strong as $B \sim 10^2 B_{\text{QED}}$, this timescale is much longer than the $\sim 10^4$ yr age of the SGR sources unless the gradient scale L of $\boldsymbol{B}$ is as small as ~ 0.2 km. As a result, the Hall term does not have a significant effect on the decay of the core magnetic field at an age of $\sim 10^4$ yr.

The effect of the Hall term on crustal field decay is more interesting. The transport of fields stronger than

$$B_{\text{frac}} \sim \theta_{\max}^{1/2} B_\mu \sim 2 \times 10^{14} \left(\frac{\theta_{\max}}{10^{-3}}\right)^{1/2} \text{ G} , \tag{48}$$

where[10]

$$B_\mu = (4\pi\mu)^{1/2} \simeq 6 \times 10^{15} \text{ G} \tag{49}$$

is qualitatively different than the transport of weaker fields. Magnetic fields weaker than B_{frac} can support high-wavenumber Hall distortions because the ions are locked into a rigid lattice. Goldreich & Reisenegger (1992) argued that dissipation of a $\sim 10^{12}$–10^{13} G magnetic field in the crust of a neutron star involves the generation of very high wavenumber Hall turbulence down to scales where ohmic dissipation is effective. By contrast, a Hall wave of sufficiently large amplitude in a field $B > B_{\text{frac}}$ stresses the crustal lattice to the point of fracture. This allows dissipation on relatively large scales where ohmic diffusion is ineffective.

These effects are best illustrated by considering a single Hall wave (eq. [44]) in a uniform magnetic field $\boldsymbol{B}_0$. A full rotation of $\delta\boldsymbol{B}$ through 2π radians is possible when $B < B_{\text{frac}}$. In stronger fields, the Maxwell stress induced by a Hall wave can be entirely compensated by hydrostatic stresses when $\delta\boldsymbol{B}_0$ lies in the vertical direction, but the rotation of the polarization vector is arrested when the horizontal component of $\delta\boldsymbol{B}$ exceeds $\delta B_{\max} \sim 4\pi\theta_{\max}\mu/B_0$. This occurs in a time

$$\Delta t_{\text{frac}} \sim \frac{\delta B_{\max}}{\delta B_0}\frac{1}{\omega} = \frac{4\pi n_e e}{cB_0 kk_\parallel}\frac{\delta B_{\max}}{\delta B_0} \tag{50}$$

and leads to a dissipation rate per unit volume of

$$\frac{(\delta B_{\max})^2}{4\pi\Delta t_{\text{frac}}} \sim \left(\frac{k_\parallel}{k}\,\theta_{\max}\right)\frac{B_\mu^2}{4\pi t_{\text{Hall}}(B, k^{-1})} , \tag{51}$$

where $t_{\text{Hall}}(B, k^{-1}) = 4\pi n_e e/cBk^2$ and we assume that the amplitude of the turbulence is large, $\delta B_0/B_0 \sim 1$. Normalizing k to the inverse of the pressure scale height ($\ell_P \simeq 0.25$ km at the base of the crust) and integrating over the volume of the crust (whose thickness is $\Delta R \simeq 0.7$ km for a model neutron star of radius 10 km; see, e.g., Lorenz, Ravenhall, & Pethick 1993), one obtains a total rate of energy release into seismic waves of

$$\frac{dE_{\text{frac}}}{dt} \simeq 2 \times 10^{34}\left(\frac{\theta_{\max}}{10^{-3}}\right)\left(\frac{B}{B_\mu}\right)(k\ell_P)^2 \text{ ergs s}^{-1} \quad (B < B_\mu) . \tag{52}$$

Note the dependence on k. The corresponding transport time is

$$t_{\text{frac}} = \left(\frac{B}{\delta B_{\max}}\right)^2 \Delta t_{\text{frac}}$$
$$= 4 \times 10^6 \left(\frac{\theta_{\max}}{10^{-3}}\right)^{-1}\left(\frac{B}{B_\mu}\right)(k\ell_P)^{-2} \text{ yr} \quad (B < B_\mu) , \tag{53}$$

[10] At the base of the crust; TD95.

assuming $k_{\|}/k = O(1)$. Setting this time equal to the decay time $t_{\rm core}$ of the core magnetic field, which is independently constrained to be 10^4–10^5 yr, one sees that a short Hall wavelength

$$\lambda \sim 0.1\left(\frac{\theta_{\rm max}}{10^{-3}}\right)^{1/2}\left(\frac{B}{B_\mu}\right)^{-1/2}\left(\frac{t_{\rm core}}{10^4\ {\rm yr}}\right)^{1/2}\ {\rm km} \quad (54)$$

is required.

There is also an upper bound to the field strength that induces fractures, in addition to the lower bound (eq. [48]). This is most easily seen from the relation between the Lagrangian displacement ξ of the crustal magnetic field, and the corresponding lattice distortion $\boldsymbol{u}$ that balances the applied Maxwell stress. We start from the Euler equation

$$\left(K + \frac{4}{3}\mu\right)\nabla(\nabla\cdot\boldsymbol{u}) - \mu\nabla\times(\nabla\times\boldsymbol{u}) = \frac{1}{4\pi}(\nabla\times\boldsymbol{B})\times\boldsymbol{B}\,, \quad (55)$$

where K is the crustal bulk modulus, μ is the shear modulus, and the magnetic field can be written as

$$\begin{aligned} \boldsymbol{B} &= \boldsymbol{B}_0 + \delta\boldsymbol{B} \\ \delta\boldsymbol{B} &= \nabla\times(\xi\times\boldsymbol{B}_0) + O(\xi^2) \quad (56)\\ &= (\boldsymbol{B}_0\cdot\nabla)\xi - \boldsymbol{B}_0(\nabla\cdot\xi) + O(\xi^2)\,. \end{aligned}$$

We first consider solenoidal distortions of the crust,

$$\nabla\cdot\boldsymbol{u} = 0\,. \quad (57)$$

These have much lower energy than compressive distortions, since $K \gg \mu$. Substituting equation (56) in equation (55), we obtain

$$\mu\nabla^2\boldsymbol{u} = -\frac{1}{4\pi}\boldsymbol{B}_0\left\{\nabla[\boldsymbol{B}_0\cdot(\nabla\times\xi)] - \nabla^2(\xi\times\boldsymbol{B}_0)\right\} + O(\xi^2)\,. \quad (58)$$

In Fourier variables $\boldsymbol{u} = \boldsymbol{u}_0 e^{i\boldsymbol{q}\cdot\boldsymbol{x}}$ and $\xi = \xi_0 e^{i\boldsymbol{k}\cdot\boldsymbol{x}}$, this equation becomes

$$-q^2\mu\boldsymbol{u}_0 = \frac{B_0^2}{4\pi}\left[(\boldsymbol{k}\times\hat{z})\xi_0\cdot(\boldsymbol{k}\times\hat{z}) - k^2\xi_0\right] + O(\xi^2)\,. \quad (59)$$

Separating ξ_0 and $\boldsymbol{k}$ into components parallel and perpendicular to $\boldsymbol{B}_0$, and making use of the identity $(\boldsymbol{k}_\perp\times\boldsymbol{B}_0)\xi_{0\perp}\cdot(\boldsymbol{k}_\perp\times\boldsymbol{B}_0) = B_0^2[k_\perp^2\xi_{0\perp} - (\xi_{0\perp}\cdot\boldsymbol{k}_\perp)\boldsymbol{k}_\perp]$, this becomes

$$q^2\mu\boldsymbol{u}_{0\perp} = \frac{B_0^2}{4\pi}[k_\|^2\xi_{0\perp} + (\xi_{0\perp}\cdot\boldsymbol{k}_\perp)\boldsymbol{k}_\perp] + O(\xi^2) \quad (60)$$

with the constraint

$$\boldsymbol{q} = \boldsymbol{k}\,. \quad (61)$$

Note that this equation makes no assumptions about whether the Lagrangian displacement vector ξ is itself divergence free.

Requiring that the crustal strain be smaller in amplitude than the original distortion of the magnetic field, $|\boldsymbol{u}| < |\xi|$, leads to an upper bound on B,

$$B < B_\mu \equiv (4\pi\mu)^{1/2} \simeq 6\times10^{15}\ {\rm G} \quad (62)$$

when $\boldsymbol{q}_\perp = 0$. Otherwise the crust is not able to support the distortion of the magnetic field, which must undergo plastic creep. Stronger magnetic fields can support Hall waves with a high wavenumber $q_\perp$ in the direction perpendicular to $\boldsymbol{B}$.

This treatment can be generalized to compressive distortions of the crust, which have strains of much smaller amplitude,

$$u = \frac{B_0^2}{4\pi[K + (4/3)\mu]}\,\xi\,. \quad (63)$$

A self-consistent equilibrium is possible only if $|\boldsymbol{u}| < |\xi|$, which implies in turn,

$$B < B_K \equiv [4\pi(K + \tfrac{4}{3}\mu)]^{1/2} \sim 1\times10^{17}\ {\rm G}\,. \quad (64)$$

How is this Hall turbulence excited in the crust? Wrinkles in the crustal magnetic field left behind after the formation of the neutron star provide some initial excitation. However, when the transport time $t_{\rm core}$ of the field through the core is shorter than equation (47), the dominant source of Hall turbulence in the crust is the diffusive motion of the magnetic field through the core. The crust encompasses only a fraction of the volume and magnetic energy of the neutron star, and so field lines that thread both the core and crust are forced through the crust. Short-wavelength Hall waves of frequency equation (46) comparable to $t_{\rm core}^{-1}$ are excited just above the crust-core boundary and then propagate upward into the crust. In this manner, we expect that a large portion of the crustal magnetic field develops short-wavelength Hall turbulence (Fig. 6).

We now relate the drift rate of the mean crustal field to the properties of the small-scale Hall turbulence. The Lagrangian displacement of the field at the top of the core integrated over a time interval δt is $\xi \simeq \boldsymbol{v}\,\delta t$. The corresponding displacement in the crust is a combination of a large-scale component $\langle\xi_c\rangle$ and a small-scale component $\delta\xi_c$ associated with Hall waves. The mean displacement $\langle\xi_c\rangle$ is generated by $\delta\xi_c$ and lags the core displacement by a distance $\sim(\delta B_{\rm max}/B_0)\lambda$,

$$\frac{\langle\xi_c\rangle}{\lambda} \simeq \theta_{\rm max}\left(\frac{B_0}{B_\mu}\right)^{-2}\frac{\boldsymbol{v}}{v}\,. \quad (65)$$

3.5. *Alfvén Wave Emission*

Now let us consider the size and energy of crustal fractures. Although most of the available magnetic field energy

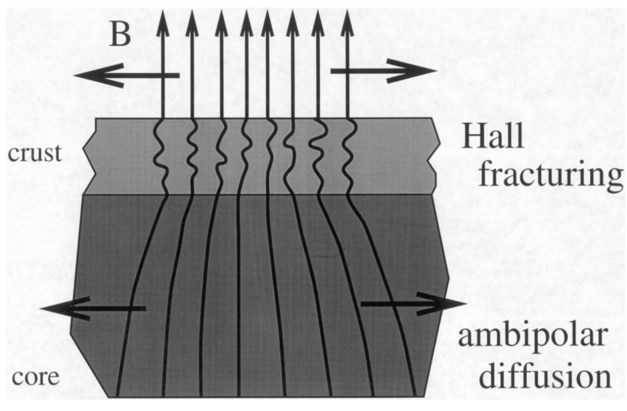

FIG. 6.—Transport of the magnetic field through the crust, driven by ambipolar diffusion in the core. Excitation of small-scale Hall turbulence in the crust causes multiple small-scale fractures when $B_\mu > B > \theta_{\rm max}^{1/2} B_\mu$.

in the core of a neutron star is released in the form of neutrino radiation, a sizable fraction of the magnetic energy in the crust is converted to seismic waves if the flux density lies in the range

$$\theta_{\max}^{1/2} B_\mu \lesssim B \lesssim B_\mu \tag{66}$$

(see eqs. [48] and [64]). Transport of the crustal field occurs by multiple small fractures of the crust by Hall waves with a characteristic wavelength λ (eq. [54]). These shear waves then couple directly to magnetospheric Alfvén modes (Blaes et al. 1989).

Given that the mean field is transported through the core on a timescale $t_{\rm core}$, the energy released in each fracture is characteristically much smaller than the energy released in an SGR burst,

$$\Delta E_{\rm frac} \sim \frac{B_{\max}^2}{4\pi} \lambda^3 \sim 1 \times 10^{36} \left(\frac{\theta_{\max}}{10^{-3}}\right)^{7/2} \times \left(\frac{B}{B_\mu}\right)^{-7/2} \left(\frac{t_{\rm core}}{10^4\ {\rm yr}}\right)^{3/2} \ {\rm ergs} \quad (B < B_\mu) . \tag{67}$$

Note the strong dependence on $\theta_{\max}$.

In addition to the short-wavelength Hall fractures driven by the ambipolar drift through the core, the crust will also undergo larger fractures on a scale comparable to the crust thickness ΔR_c. In the model developed in TD95, these larger scale fractures trigger soft gamma repeater bursts. They will also lead to plate tectonic motion analogous to that envisaged by Ruderman (1991) in the crust of a pulsar whose spin period changes with time, but in a magnetar, magnetic field lines rather than superfluid vortex lines are the dominant sources of crustal stress.

What are the relative amounts of energy released by large-scale and small-scale fractures? When the solenoidal mode of ambipolar diffusion is much faster than the irrotational mode, the charged particle flux $n_e \boldsymbol{v}$ in the core is to a first approximation irrotational on a timescale $t_{\rm amb}^{irr}$. The Lagrangian displacement ξ_c of the crustal magnetic field is proportional to $\boldsymbol{v}$, and it is the rotational component of ξ_c that is responsible for shearing the crust (eq. [55]). Although $\boldsymbol{v}$ itself is not entirely irrotational, because n_e has a radial gradient, the *radial* component of $\nabla \times \boldsymbol{v}$ still does vanish to first order, since[11]

$$\nabla \times (n_e \boldsymbol{v}) \simeq n_e \nabla \times \boldsymbol{v} + \frac{\partial n_e}{\partial r} \hat{r} \times \boldsymbol{v} = 0 . \tag{68}$$

We denote by $\boldsymbol{v}_\perp$ the two-dimensional projection of $\boldsymbol{v}$ onto a plane tangent to the surface of the star. Averaging $\boldsymbol{v}_\perp$ over a section of the crust of area $\sim(\Delta R_c)^2$ yields a small curl

$$|\nabla_\perp \times \boldsymbol{v}_\perp| \sim \left(\frac{\Delta R_c}{R_\star}\right)^2 \frac{v_\perp}{R_\star} \tag{69}$$

because of the curvature of the crust. Averaging over a smaller patch of crust yields a smaller curl. In sum, we estimate the ratio of the total energy released in SGR bursts to that released in small-scale Alfvén excitations as

$$\frac{\langle \dot{E}({\rm SGR}) \rangle}{\langle \dot{E}({\rm A}) \rangle} \sim \left(\frac{\Delta R_c}{R_\star}\right)^2 \sim 10^{-2} \tag{70}$$

[11] Temporal and spatial gradients in n_e induced by the magnetic field are smaller by a factor $\sim B^2/8\pi P$ and can be ignored.

when $t_{\rm amb}^s \ll t_{\rm amb}^{irr} \sim t$. Assuming that the core magnetic field decays substantially at age t, the Alfvén wave luminosity is

$$L_{\rm A} \simeq \frac{4\pi R_\star^2 \Delta R_c}{t} \frac{B_c^2}{8\pi} = 6 \times 10^{36} \times \left(\frac{B_c}{B_\mu}\right)^2 \left(\frac{t}{10^4\ {\rm yr}}\right)^{-1} \left(\frac{\Delta R_c}{1\ {\rm km}}\right) {\rm ergs\ s^{-1}} . \tag{71}$$

As before, B_c is the crustal field strength. When $B_c \lesssim B_\mu \sim 6 \times 10^{15}$ G and $t \sim 10^4$ yr, this is comparable to the particle luminosity inferred for SGR 1806−20 (Appendix A).

This low-amplitude Alfvén wave emission is suppressed when $B_c > B_\mu$, because the crust undergoes a plastic deformation in such a strong magnetic field.

3.6. *Quiescent X-Ray Emission*

A basic observable signature of a magnetar is the quiescent X-ray emission powered by the internal magnetic dissipation. Here, we present further details of the calculation presented in TD93b. Usov (1984) considered the heating of an old, relatively cold neutron star by a much weaker magnetic field, whose decay rate was taken as a fixed parameter, but did not solve self-consistently for the time evolution of both T and B. Urpin & Shalybkov (1995) have also noted that ambipolar diffusion can heat the core of a neutron star. However, they neglect the stable stratification of the neutron star core (Reisenegger & Goldreich 1992) and assume that ambipolar diffusion is limited primarily by proton-neutron drag, which we have argued is not the case for core temperatures in the range of interest (§ 3.2.).

The surface X-ray emission is easily estimated from the core temperature (eq. [39]) and the core-surface temperature relation derived by Van Riper (1988), which we parameterize as

$$T_{\rm eff} = 1.3 \times 10^6 \left(\frac{T_c}{10^8\ {\rm K}}\right)^{5/9} {\rm K} \quad (B \sim 10^2 B_{\rm QED}) . \tag{72}$$

The ratio $T_c/T_{\rm eff}$ is only weakly dependent on the magnetic flux density in the surface layers of the neutron star, being suppressed by a factor ~ 0.6 at $B \sim 10 B_{\rm QED}$ from the value at $B = 0$. Equation (72) is valid only for $T_{\rm eff} \gtrsim 1.5 \times 10^6 (B/10 B_{\rm QED})^{0.3}$ K because of the large Coulomb correction to the pressure in the outer crust (Fig. 29 of Van Riper 1988). The surface X-ray flux is, neglecting the gravitational redshift,

$$\begin{aligned} L_{\rm X}(t) &= 1.2 \times 10^{35} \left(\frac{T_c}{6 \times 10^8\ {\rm K}}\right)^{2.2} R_{\star 6}^2\ {\rm ergs\ s^{-1}} \\ &= 5 \times 10^{34} \left(\frac{t}{10^4\ {\rm yr}}\right)^{-0.32} \\ &\quad \times \left(\frac{\rho_{15}}{0.7}\right)^{0.11} \left(\frac{Y_e}{0.05}\right)^{0.32} R_{\star 6}^2\ {\rm ergs\ s^{-1}} \end{aligned} \tag{73}$$

if the magnetic field decays by a factor ~ 2 at age t and the core temperature is given by equation (39). Here ρ and Y_e are the characteristic density and electron fraction at which most of the magnetic dissipation takes place.

The X-ray luminosity (eq. [73]) is indeed comparable to the quiescent emission detected from the two SGR sources

0526−66 and 1806−20 and from the anomalous X-ray pulsar 1E 2259+586, as we discuss further in § 4. A higher X-ray flux could be generated at the same age if the core neutrons formed a superfluid (§ 3.8).

The corresponding ratio of surface X-ray luminosity to core neutrino luminosity (eq. [37]) is

$$\frac{L_X(t)}{L_\nu(t)} = 9 \times 10^{-3}\left(\frac{t}{10^4\ \mathrm{yr}}\right)^{0.83}\left(\frac{\rho_{15}}{0.7}\right)^{-0.94}\left(\frac{Y_e}{0.05}\right)^{-0.83} R_{\star 6}^{-1} . \quad (74)$$

Van Riper (1991) has calculated the surface X-ray flux emerging from a heat source in the interior of an otherwise cold neutron star and finds that the X-ray luminosity saturates at $L_X \sim 10^{35}$ ergs s^{-1} because of rapid neutrino cooling. In the above calculation, neutrino cooling limits L_X to a similar value at an age of $\sim 10^4$ yr. Because the release of magnetic energy begins to dominate secular cooling only at an age of $\sim 10^3$ yr (see eq. [39]), equation (73) cannot be much larger than the X-ray luminosity of a cooling neutron star with $B = 0$. Inspection of equation (74) shows that the surface photon cooling begins to dominate the core neutrino cooling at an age

$$t(\text{photon cooling}) \simeq 2 \times 10^6\left(\frac{\rho_{15}}{0.7}\right)^{1.1}\left(\frac{Y_e}{0.05}\right) R_{\star 6}^{1.2}\ \mathrm{yr} , \quad (75)$$

after which the temperature of the star begins to drop rapidly. As we discuss in the next section, suppression of thermal conduction across the magnetic field may allow parts of the core to remain hot even when $t > t$(photon cooling) (see also TD93b).

3.7. *Anisotropic Electron Thermal Conduction: Effects on Cooling*

The calculation of the anomalous surface photon flux in § 3.5 assumes that the heat generated in the core by the diffusing magnetic field is freely conducted to the surface. The strong magnetic field will, in fact, suppress the electron thermal conductivity κ_e in the direction perpendicular to $\boldsymbol{B}$ (see, e.g., Hernquist 1985),

$$\frac{\kappa_e(\perp)}{\kappa_e(B=0)} \simeq \left(\frac{eB\tau_k}{\mu_e}\right)^{-2} \quad (76)$$

while leaving the conductivity parallel to $\boldsymbol{B}$ essentially unchanged, $\kappa_e(\|) \simeq \kappa_e(B=0)$. Neglecting the effects of proton superconductivity in the core (which is reasonable for $B \gtrsim B_1 \sim 10^2 B_{\mathrm{QED}}$, where B_1 is the lower critical field strength; Easson & Pethick 1977) the mean free path of an electron near the Fermi surface is

$$\tau_k = \frac{3\pi}{4\alpha^2}\,\mu_e^{-1} . \quad (77)$$

Here we set the Coulomb logarithm to unity. The electron chemical potential is $\mu_e = (3\pi^2\mu_e)^{1/3} = 190\rho_{15}^{1/3}(Y_e/0.05)^{1/3}$ MeV, and so the suppression factor is

$$\frac{\kappa_e(\perp)}{\kappa_e(B=0)} \simeq 1.8 \times 10^{-4}\left(\frac{B}{10^2 B_{\mathrm{QED}}}\right)^{-2}\left(\frac{\rho}{\rho_{nuc}}\right)^{4/3}\left(\frac{Y_e}{0.05}\right)^{4/3} . \quad (78)$$

The magnetic field in the core of a magnetar will have spatial gradients, which create gradients in the heating rate by ambipolar diffusion. We now estimate the effectiveness of electron thermal conduction at erasing temperature gradients both parallel and perpendicular to $\boldsymbol{B}$.

A temperature gradient on a scale L causes a maximal rate of energy loss (or gain) per unit volume,

$$\dot{U}_{\mathrm{cond}}(\|, \perp) \sim \frac{\kappa_e(\|, \perp)T}{L^2} . \quad (79)$$

The thermal conductivity of a normal, degenerate *n-p-e* plasma is (see, e.g., Urpin & Yakovlev 1980)

$$\kappa_e(B=0) = \frac{\pi^2}{3}\frac{Tn_e\tau_\kappa}{\mu_e} = \frac{\pi}{12\alpha^2}\,T\mu_e . \quad (80)$$

Including the suppression factor (77) to conduction perpendicular to $\boldsymbol{B}$ and using the equilibrium relation (eq. [31]) between T and B, one finds

$$\frac{\dot{U}_{\mathrm{cond}}(\|)}{\dot{U}_{\mathrm{URCA}}} \simeq \left[\frac{B}{B_{\mathrm{cond}}(\|)}\right]^{-12} , \quad (81)$$

and

$$\frac{\dot{U}_{\mathrm{cond}}(\perp)}{\dot{U}_{\mathrm{URCA}}} \simeq \left[\frac{B}{B_{\mathrm{cond}}(\perp)}\right]^{-14} , \quad (82)$$

where

$$B_{\mathrm{cond}}(\|) = 5.9 \times 10^{15}\rho_{15}^{17/36}\left(\frac{Y_e}{0.05}\right)^{19/36} L_6^{-1/6}\ \mathrm{G} , \quad (83)$$

and

$$B_{\mathrm{cond}}(\perp) = 3.5 \times 10^{15}\rho_{15}^{1/2}\left(\frac{Y_e}{0.05}\right)^{23/42} L_6^{-1/7}\ \mathrm{G} . \quad (84)$$

From the scaling solution (eq. [35]) for the core magnetic field, the corresponding ages are

$$t_{\|} \simeq 1 \times 10^4\rho_{15}^{13/18}\left(\frac{Y_e}{0.05}\right)^{11/8}\left(\frac{L_6}{0.3}\right)^{7/3}\ \mathrm{yr} , \quad (85)$$

for conduction parallel to $\boldsymbol{B}$, and

$$t_{\perp} \simeq 1 \times 10^7\rho_{15}^{1/3}\left(\frac{Y_e}{0.05}\right)^{1/3}\left(\frac{L_6}{0.3}\right)^{2}\ \mathrm{yr} , \quad (86)$$

for conduction perpendicular to $\boldsymbol{B}$.

The thermal structure of the core depends crucially on the *connectivity* of the magnetic field. When B is stronger than $B_{\mathrm{cond}}(\perp)$ and neutron thermal conduction can be neglected ($T \ll T_{\mathrm{cr}}$), regions of the core containing closed magnetic field lines are thermally isolated from their surroundings up to an age (eq. [86]). Such regions will remain magnetically active even after regions of the core that are connected to the surface of the neutron star have frozen out. For example, if the neutron star has an age greater than equation (75), where surface photon cooling begins to dominate core neutrino cooling, but less than equation (86), then part of the core can remain much hotter than the crust-core boundary. Note also that even thermal conduction along the magnetic field lines is not sufficient to erase temperature gradients created by irregularities in the magnetic heating rate, when B is stronger than $B_{\mathrm{cond}}(\|)$.

3.8. *Effects of Neutron Superfluidity and Kaon Condensation*

Neutron superfluidity has two important effects on the evolution of a strong core magnetic field: both the modified URCA cooling rate and the ambipolar diffusion rate[12] are suppressed by a factor $\sim e^{-\Delta/T}$, where Δ is the gap energy. Estimates of the peak critical temperature for $^3P_2$ neutron pairing in the core of a neutron star range from $\sim 7 \times 10^8$ K (Takatsuka 1972) to $\sim 3 \times 10^9$ K (Hoffberg et al. 1970; Sauls & Serene 1978), with the temperature vanishing below about nuclear matter density. The gap energy is typically a factor ~ 2 larger. When T_c exceeds the temperature $T_{\rm trans}$ (eq. [19]), the irrotational mode of ambipolar diffusion is limited by pressure gradient forces at $T \lesssim T_c$.

The net result is that the equilibrium relation (eq. [31]) between T and B is not changed to first order by neutron superfluidity. The rates of both ambipolar diffusion and neutrino cooling are limited by the modified-URCA reaction, and so the dependence on Δ cancels. Nonetheless, the characteristic strength of a magnetic field that decays at a given age does increase, with the result that *the main observable effect of core neutron superfluidity on the decay of the core magnetic field is to increase the maximum core temperature that can be maintained by ambipolar diffusion at a given age and thus to increase the anomalous surface X-ray flux and Alfvén wave flux powered by this decay.*

Let us give a numerical example. If the neutrons are normal, then the core temperature of a magnetar whose field decays at an age of 10^4 yr is $T_{\rm eq}({\rm normal}) = 5 \times 10^8$ K [eq. (39)]. If instead the neutrons are superfluid with $\Delta = 10^{10}$ K, then the equilibrium temperature increases to $T_{\rm eq}({\rm superfluid}) = 1.3 \times 10^9$ K. Alternatively, if $\Delta = 3 \times 10^9$ K, then $T_{\rm eq}$ only increases to $T_{\rm eq}({\rm superfluid}) = 8 \times 10^8$ K. The magnetic field generated by a fast, transient dynamo in a newborn neutron star probably is highly intermittent, being concentrated into strong, isolated flux ropes (TD93a). This raises the possibility that neutron superfluidity is suppressed inside the ropes but not in the medium between ropes.

Nonetheless, the anomalous surface X-ray flux (§ 3.7) cannot be increased arbitrary by raising the $^3P_2$ neutron gap energy. Neutrino bremsstrahlung emission from the crust is not suppressed by neutron superfluidity. The corresponding neutrino luminosity is

$$L_\nu = 5 \times 10^{35} T_{c9}^{6.8} \left(\frac{M_{\rm cr}}{10^{-2}\,M_\odot}\right) \text{ ergs s}^{-1} \tag{87}$$

near $T \sim 10^9$ K, assuming $Y_e = 0.04$ and a charge per nucleus of $Z = 30$ (Pethick & Thorsson 1994). Balancing the magnetic dissipation rate $(4\pi R_\star^3/3)(B^2/8\pi t)$ against the crustal neutrino luminosity (eq. [87]) and using the $T(B)$ relation (eq. [31]) yields the following *upper* bound on the core field strength,

$$B \lesssim 1.3 \times 10^{16} \left(\frac{t}{10^4\ {\rm yr}}\right)^{-1/10} \left(\frac{M_{\rm cr}}{10^{-2}\,M_\odot}\right)^{-1/10} \times R_{\star 6}^{3/10} \left(\frac{\rho_{15}}{0.7}\right)^{3/5} \left(\frac{Y_e}{0.05}\right)^{3/5} \text{ G}, \tag{88}$$

[12] When limited by pressure gradient forces: §3.2.

core temperature,

$$T \lesssim 2 \times 10^9 \left(\frac{t}{10^4\ {\rm yr}}\right)^{-1/5} \left(\frac{M_{\rm cr}}{10^{-2}\,M_\odot}\right)^{-1/5} \times R_{\star 6}^{3/5} \left(\frac{\rho_{15}}{0.7}\right)^{1/5} \left(\frac{Y_e}{0.05}\right)^{1/5} \text{ K}, \tag{89}$$

and surface X-ray flux

$$L_{\rm X} \lesssim 2 \times 10^{36} \left(\frac{t}{10^4\ {\rm yr}}\right)^{-0.4} \left(\frac{M_{\rm cr}}{10^{-2}\,M_\odot}\right)^{-0.4} \times R_{\star 6}^{3.2} \left(\frac{\rho_{15}}{0.7}\right)^{0.4} \left(\frac{Y_e}{0.05}\right)^{-0.4} \text{ ergs s}^{-1} \tag{90}$$

for a magnetar whose field decays at age t.

Formation of a kaon (or pion) condensate in the central core of a neutron star will rapidly accelerate the neutrino cooling rate (Kaplan & Nelson 1986; Tsuruta 1995). However, we have seen in § 3.8 that electron thermal conduction is strongly suppressed across the magnetic field. As a result, regions of the core in which the magnetic field is *not* connected to the central condensate will be prevented from undergoing rapid cooling, as long as $B > B_{\rm cond}(\perp)$ (eq. [84]) and neutron thermal conduction can be neglected ($T \ll T_{\rm cr}$).

We emphasize that rapid cooling by a kaon condensate is prevented only for relatively young neutron stars; at the age of $\sim 10^8$ that is encountered in halo models for gamma-ray bursts (see, e.g., DT92; Li & Dermer 1992; Duncan, Li, & Thompson 1993; Posiadlowski, Rees, & Ruderman 1995), one finds that $\dot{U}_{\rm cond}(\perp) \gtrsim \dot{U}_{\rm URCA}$.

4. APPLICATION TO THE SGRs AND AXPs

4.1. (*Pulsating*) *Quiescent X-Ray Emission*

A very strong magnetic field $B \sim 10^2 B_{\rm QED}$ diffuses out of the core of a neutron star on a timescale of $\sim 10^4$ yr (eq. [33]). Thermal energy is conducted from the heated core to the surface and powers an anomalously high X-ray flux (TD93a; eq. [73]). The photon luminosity is limited to $L_{\rm X} \sim 10^{35}$–10^{36} ergs s^{-1} by neutrino cooling at an age of $\sim 10^4$ yr (depending on the superfluid state of the core neutrons). This compares favorably with the quiescent emission observed from the AXPs and from two of the SGR sources. The magnetic field also induces multiple small-scale fractures of the crust (each fracture releasing orders of magnitude less energy than a typical SGR burst: § 3.5). The resulting Alfvén wave luminosity depends sensitively on the ratio B/B_μ. When $B \gg B_\mu$, the crust undergoes a plastic deformation, and seismic activity is suppressed. The core magnetic field, which decays at an age of $\sim 10^4$ yr, is, by coincidence, nearly the same as B_μ. Thus, the ratio of thermal to nonthermal X-ray output from a magnetar of this age can, in principle, cover a wide range.

Let us compare these results with the observations in more detail. The X-ray spectrum of 1E 2259+586 appears to be dominated by a blackbody component of temperature $\simeq 0.4$ keV (Corbet et al. 1995; Baykal & Swank 1996). The observed luminosity of $L_{\rm X} \simeq 0.5 \times 10^{35}(D/3\ {\rm kpc})^2$ ergs s^{-1} (assuming isotropic emission: Iwasawa et al. 1992; Baykal & Swank 1996) is consistent with emission in one polarization mode from a neutron star of radius 10 km at a distance of 1.5 kpc, or equivalently with emission from two polar hot spots of radius $7(D/3\ \text{kpc})$ km. The implied core temperature is $T_{\text{core}} \sim 6 \times 10^8$ K using relation (72). From the $T(B)$ relation (31), one deduces a core magnetic field strength $B \simeq (6–7) \times 10^{15}$ G, which is comparable to B_μ. The age of supernova remnant CTB 109 associated with 1E 2259+586 is $\sim 1 \times 10^4$ yr (Wang et al. 1992). If the magnetic field in that source has a similar decay time, then equation (73) predicts $L_X \simeq 5 \times 10^{34}$ ergs for a *n-p-e* degenerate plasma, which is comparable to the observed value.

The X-ray light curve of a rotating magnetar depends on the distribution of the heat flux and Alfvén wave flux over its surface. The equilibrium core $T(B)$ relation (eq. [31]) combined with the T_{eff}-T_c relation (eq. [72]) yields a surface heat flux that is a strong function of B,

$$F_X \sim \sigma_{\text{SB}} T_{\text{eff}}^4 \propto T_c^{2.2} \propto B^{4.4} . \tag{91}$$

Moreover, the heat flux is channeled *along* the magnetic field lines (§ 3.7) to a small enough depth in the crust that smoothing of gradients in the heat flux perpendicular to $\boldsymbol{B}$ by radiative transport can be neglected in calculating the distribution of F_X over the surface of the star. This means that if the dipolar magnetic field lines are concentrated in two strong polar spots, then the surface X-ray flux is even more strongly localized. The effective temperature of *one* polarization mode (the extraordinary mode) with a low absorption cross section is related to the radius of the polar spots by

$$T_{\text{eff}} \simeq 0.77\left(\frac{L_X}{10^{35}\ \text{ergs s}^{-1}}\right)^{1/4}\left(\frac{R_{\text{spot}}}{3\ \text{km}}\right)^{-1/2} \text{keV} . \tag{92}$$

Similar estimates can be made for the SGR sources. The age of the LMC supernova remnant N49 associated with SGR 0526−66 is similar to that of CTB 109 ($\sim 5 \times 10^3$ yr; Vancura et al. 1992). Note that the decay time of the core magnetic field is increased by neutron superfluidity, with the result that a stronger magnetic field and a *higher* temperature are possible at a fixed age (§ 3.8). The quiescent X-ray luminosity of the compact source in N49 ($L_X \sim 7 \times 10^{35}$ ergs s^{-1}; Rothschild et al. 1993, 1994), although several times larger than that of 1E 2259+586, could be contaminated by a hot spot in the nebular emission.

Comparison with SGR 1806−20 is more problematic, since the X-ray emission from that source appears to be nonthermal (Murakami et al. 1994; Sonobe et al. 1994). The nonthermal shape of the spectrum is probably closely connected with the fact that the surrounding SNR is a nonthermal radio plerion (Kulkarni et al. 1994; Vasisht et al. 1995). We have suggested a mechanism for powering the plerion other than rotation: a quasi-steady stream of low-amplitude Alfvén waves triggered by diffusion of the magnetic field through the neutron star crust (TD95; § 3.5). These Alfvén waves would be effective at accelerating nonthermal particles, thereby Comptonizing softer X-ray photons, but a calculation of the resulting photon spectrum is beyond the scope of this paper.

If the quiescent X-ray emission of the SGR sources is powered by a strong, decaying magnetic field, then the fact that the L_X of SGR 0526−66 exceeds that of SGR 1806−20 suggests that 0526−66 has a stronger magnetic field. This is consistent with the fact that the bursts emitted by SGR 0526−66 have harder spectra (by a factor $\sim$1.3–1.5 in temperature: Mazets et al. 1982; Fenimore et al. 1994) and higher luminosities. In the radiative model developed in TD95, the strong magnetic field suppresses the electron scattering opacity and increases the limiting luminosity of the source (see also Joss & Li 1978; Paczyński 1992).

SGR 1806-20 has undergone an order of magnitude more observed bursts than SGR 0526−66. This relatively high burst rate may be physically connected to the fact that SGR 1806−20 is also an *active* source of relativistic particles (TD95; § 2). The energy released in the form of large-scale fractures of the crust (that can trigger SGR bursts) should increase monotonically with the energy released in the form of small-scale fractures (that power the quasi-steady Alfvén wave emission). The Alfvén wave luminosity given by equation (71) is very close to the particle luminosity inferred for SGR 1806−20 (Appendix A) if the distance of the source is $\sim$8 kpc and $B \sim B_\mu \simeq 6 \times 10^{15}$. Note that the lower burst rate of SGR 0526−66 is consistent with that source having a *stronger* magnetic field, if the internal flux density exceeds B_μ and the crust undergoes a plastic deformation (§ 3.4; TD95).

4.2. *Glitches and Variability in L_X*

Until now, we have worked under the approximation that the magnetic energy of the neutron star is released steadily. Sudden fractures of the neutron star crust can release enough energy to power SGR bursts (TD95), but it is plausible that transient surges of magnetic dissipation occur a range of timescales greater than the Alfvén crossing time of the star ($\sim 0.1 B_{15}^{-1}$ s) but less than its age ($\sim 10^4$ yr). For example, if the magnetic field at the base of the crust is stronger than $B_\mu \simeq 6 \times 10^{15}$ G, then the crust undergoes a plastic creep instead of fracturing. In this section, we examine two observational consequences of such surges in the dissipation rate: glitches and variations in the surface X-ray flux.

Glitches are an almost certain by-product of SGR bursts in the magnetar model. When a patch of the crust (of size $\Delta\ell$) fractures under the applied magnetic stresses, the crustal lattice and the crustal $^1S_0$ neutron superfluid suddenly develop a large angular velocity difference $\Delta\Omega \sim (\mu/\rho)^{1/2}/\Delta\ell \sim 10^3(\Delta\ell_5)^{-1}$ s^{-1}, which should be large enough to unpin the superfluid neutron vortex lines from the lattice (TD93a, § 14.5). If the magnetic field undergoes a slower plastic deformation (as should happen when $B > B_\mu$ in the crust), then a glitch may also result. This is because the internal magnetic energy of a magnetar exceeds the rotational energy of the crustal superfluid by a large factor $\sim 1 \times 10^6 (P/7\ \text{s})^2 (B/B_\mu)^2$, which is the opposite of the inequality encountered in young radio pulsars. As a result, the superfluid vortex lines are dragged with the crustal lattice, and the interchange of two patches of the crust with different densities of vortex lines may create a large enough local angular velocity lag to unpin the vortex lines. Finally, a sudden surge in the magnetic dissipation rate heats the crust. Such a temperature increase can greatly increase the creep rate of the vortex lines through the lattice and effectively trigger a glitch (Link & Epstein 1995).

The magnitude of the glitches triggered in a slowly rotating magnetar can be quite large. Assuming that a fraction ϵ_c of the crustal superfluid unpins and decreases in angular velocity by $\Delta\Omega_n$, the neutron star is observed to spin up by a fractional amount

$$\frac{\Delta P}{P} \sim -0.11\epsilon_c\left(\frac{I_n}{10^{-2} I}\right)\left(\frac{|\Delta\Omega_n|}{10\ \text{s}^{-1}}\right)\left(\frac{P}{7\ \text{s}}\right) . \tag{93}$$

Here $I_n/I \sim$ (1–2) $\times 10^{-2}$ is the fraction of the moment of inertia of the star in the crustal superfluid (Lorenz et al. 1993). Because the neutron star is spinning slowly (with $\Omega = 2\pi/P$ less than the maximum angular velocity difference $\Delta\Omega_{\max} \sim$ 1–100 s^{-1} at which the vortex lines unpin spontaneously) parts of the crustal superfluid may contain dense bundles of vortex lines and continue to spin much more rapidly than the surface of the star.

For example, if the vortex lines unpin in a patch of the crust of size $\sim$(1 km)^2, then $\epsilon_c \sim 10^{-3}$ and $\Delta P/P \sim -1 \times 10^{-4}$. More realistically, one might scale to the Crab pulsar, since the internal temperature (eq. [39]) inferred for a magnetar of age $\sim 10^4$ yr is close to that predicted by standard cooling models for a neutron star of age $\sim 10^3$ yr (Tsuruta 1995). Then the maximum glitch amplitude expected from a magnetar is

$$\frac{\Delta P}{P} \sim -4 \times 10^{-8} \times \frac{P_{\text{magnetar}}}{P_{\text{Crab}}} \sim -1 \times 10^{-5} . \quad (94)$$

Here $\Delta P/P \sim -4 \times 10^{-8}$ is the largest amplitude glitch detected from the Crab pulsar (Lohsen 1981).

Variations in the surface X-ray flux are driven by fluctuations in the internal magnetic dissipation rate. The timescale of these flux variations depends on whether the energy is transported by thermal conduction from the core to the surface or by low-amplitude Alfvén waves into the magnetosphere.

Fluctuations in the Alfvén wave flux will almost instantly lead to variations in the X-ray flux. By contrast, the thermal conduction time from a density greater than $\sim 10^{12}$ g cm^{-3} to the surface of a neutron star is quite long, $t_{\text{cond}} \sim 2 \times 10^7$ s at a surface temperature of $T_{\text{eff}} = 3 \times 10^6$ K. [We extrapolate the detailed calculations of Van Riper, Epstein, & Miller 1991 which were given for $T_{\text{eff}} \sim (0.4\text{–}1) \times 10^6$ K.] As a result, small-amplitude fluctuations in the *core* dissipation rate, on a timescale shorter than ~ 1 yr, are smoothed out. Large-amplitude fluctuations in the dissipation rate on this short a timescale will yield detectable changes in L_X but only if the total energy released (above the background dissipation rate) exceeds

$$\Delta E > t_{\text{cond}} L_\nu \sim 1 \times 10^{44} \text{ ergs} , \quad (95)$$

where we use $L_\nu \sim 4 \times 10^{36}$ ergs s^{-1} as appropriate to a magnetar of age $\sim 10^4$ yr (eq. [37]).

If this energy is released in the core, then all but a fraction $\sim 10^{-2}$ is converted to neutrino radiation (cf. eq. [74]). If this energy is released in the crust, then new estimates of the crustal bremsstrahlung neutrino emissivity (Pethick & Thorsson 1994) suggest that the direct neutrino losses from the crust are small. At an internal temperature of 5.5×10^8 K (which corresponds to $L_X = 10^{35}$ ergs s^{-1} from eq. [73]), one has $L_\nu(\text{bremss}) = 4 \times 10^{33}(M_{\text{cr}}/10^{-2}\ M_\odot)$ ergs s^{-1}, where M_{cr} is the mass of the crust. However, a doubling of L_X requires a $\sim 35\%$ increase in T_c, which corresponds to a heat input to the crustal lattice of

$$\Delta E_{\text{th}} \simeq \frac{3Y_e}{2Z}\left(\frac{M_{\text{cr}}}{m_p}\right)\Delta T_c \sim 6 \times 10^{44}\left(\frac{M_{\text{cr}}}{10^{-2}\ M_\odot}\right) \text{ergs}$$
$$(\delta L_X = 0.5 \times 10^{35} \text{ ergs s}^{-1}) . \quad (96)$$

Here we have used $Y_e = 0.04$ and $Z = 30$ for the charge per nucleon. This thermal energy is still ~ 600 times larger than the excess X-ray energy radiated over a time t_{cond}, because most of the heat is conducted into the core.

We conclude that a significant upward shift in L_X, driven by thermal conduction out of the core (or lower crust) on a timescale $t_{\text{cond}} \sim 1$ yr, requires an energy input comparable to the energy released in the 1979 March 5 burst ($\sim 5 \times 10^{44}$ ergs assuming isotropic emission: Mazets et al. 1982). In other words, such a delayed afterglow emission is predicted by almost any model for the March 5 event in which comparable mechanical energy is dissipated inside the star. (The magnetospheric emission model developed in TD95 also makes the prediction of a much more luminous afterglow of $L_X \sim 10^{39}$ ergs s^{-1} on a timescale comparable to the ~ 200 s duration of the burst because of heating of a thin upper layer of the crust by an external pair-photon plasma.) By contrast, if the increased X-ray flux is driven by a increase in the Alfvén wave flux, then the energetic requirements are less severe.

The X-ray pulsar 1E 2259+586 provides an opportunity to test these ideas since, unlike SGR 0526−66, X-ray pulsations are detected and its spin-down history is (partly) known. This source exhibited a moderate increase in L_X, from 0.4×10^{35} ergs s^{-1} to 1×10^{35} ergs s^{-1}, between 1989 December and 1990 August (Iwasawa et al. 1992). The X-ray luminosity was slightly lower when the source was reobserved by BBXRT in 1990 December and appeared to have returned to the 1989 level when observed by *ASCA* in 1993 (Corbet et al. 1995). The duration of the enhanced X-ray emission therefore is consistent with the timescale for thermal conduction from the deep crust to the surface of the neutron star (for $T_{\text{eff}} \sim 4 \times 10^6$ K). The X-ray light curve maintained almost the same shape when L_X increased, with both the main pulse and interpulse growing in amplitude. Such an upward shift in the light curve could, of course, be explained naturally by an increase in the rate of mass accretion. In the magnetar model, one requires that comparable energy is dissipated near both magnetic poles (where the magnetic dissipation and surface X-ray flux is concentrated). This is achieved quite naturally if the thermal component of the spectrum is powered mainly by energetic particles that are accelerated by Alfvén waves at a radius $R \sim c/v_A$ and flow back to heat the polar caps of the neutron star. (In this case, the timescale on which L_X varies is only by coincidence comparable to t_{cond}.)

There is tentative evidence from the spin-down history of 1E 2259+586 (Fig. 1 of Iwasawa et al. 1992) that the neutron star underwent a glitch of amplitude $\Delta P/P \simeq -3 \times 10^{-6}$ between 1 and 3 years *before* L_X was observed to increase[13] (Usov 1994). Note that this is in the range of glitch amplitudes expected in young magnetars (eqs. [93] and [94]). Furthermore, thermal conduction to the surface does yield a time delay before the onset of the enhanced X-ray emission which is comparable to its duration (Van Riper et al. 1991).

Thus a glitch is a natural consequence of a rearrangement of the magnetic field of a magnetar. The occurrence of a glitch in an isolated massive white dwarfs (§ 2.3) requires more special conditions (Usov 1994). In particular, spin-down glitches driven by a solid body fracture are difficult to

[13] A brief note of this possibility was made independently in Duncan & Thompson (1994).

understand in a white dwarf formed via merging at time $t_{\rm SNR} \sim 10^4$ yr ago (Paczyński 1990), since such a star may not have cooled sufficiently to crystallize. Only for pure iron composition is such rapid crystallization marginally possible (Usov 1994).

The main problem with invoking a *sudden* rearrangement[14] of the magnetic field of 1E 2259+586 as the trigger for both a luminosity fluctuation and a glitch is that this source did not emit an X-ray burst even remotely approaching in energy or brightness the March 5 event. (Note also that SGR 0526−66 is a factor ~10 more distant.) The neutron star crust would necessarily have undergone a plastic deformation instead of fracturing.

Finally, we note that the rotational energy released by a large glitch such as equation (94) is at most

$$\Delta E_{\rm glitch} \simeq I\Delta\Omega\,|\,\Delta\Omega_n\,| \lesssim I\Delta\Omega\Delta\Omega_{\rm max}$$

$$\sim 1 \times 10^{41}\left(\frac{P}{7\ {\rm s}}\right)^{-1}\left(\frac{\Delta\Omega/\Omega}{10^{-5}}\right)\left(\frac{\Delta\Omega_{\rm max}}{10\ {\rm s}^{-1}}\right)\ {\rm ergs}\ . \quad (97)$$

The resulting perturbation on a surface luminosity of $L_{\rm X} \sim 10^{35}$ ergs s^{-1} is negligible, especially when neutrino losses are taken into account. Van Riper et al. (1991) found that glitches in fast young pulsars could trigger noticeable afterglow, but only for surface $L_{\rm X}$ a factor $\sim 10^2$–10^3 smaller.

5. CONCLUSIONS AND PREDICTIONS

The most pressing question regarding the SGR and AXP sources, one that still needs a definitive observational test, is whether these sources are *accreting* neutron stars or instead *magnetars* with decaying magnetic fields. The detection of quiescent X-ray emission from both SGR 0526−66 and SGR 1806−20 would seem to suggest, at first sight, that these sources are accreting. However, the detection of large particle outflow from SGR 1806−20 (more than enough to blow away the mass that is needed to power the quiescent X-rays) provides direct evidence that that source is *not* an accretor. A further complication that should be kept in mind is that these two SGR sources may not fit into a uniform class. Only one of them has emitted a superburst (SGR 0526−66), only one of them is surrounded by a detectable nonthermal radio plerion (SGR 1806−20), and only one of them (SGR 1806−20) has a luminous companion (Kulkarni et al. 1995; Van Kerkwijk et al. 1995). Nonetheless, the relatively short ($\Delta t \sim 0.1$ s), extremely luminous ($L \sim 10^3$–$10^4 L_{\rm edd}$), and relatively hard repeat bursts that these sources emit are similar enough to suggest that these sources share some basic parameter (such as magnetic field strength) that differs markedly from ordinary X-ray burst sources.

The key point of this paper is that once a strong magnetic field is invoked to explain the various extreme properties of SGR bursts (DT92; Paczyński 1992; TD95), the decay of the magnetic field itself can plausibly account for the quiescent X-ray and particle emission from these sources. Neutrino losses from the core cause the surface X-ray flux to saturate at $L_{\rm X} \sim 10^{35}$–10^{36} ergs s^{-1} at an age $\sim 10^4$ yr. The star should be a copious source of low-amplitude Alfvén waves if $B \lesssim B_\mu \sim 6 \times 10^{15}$ G at the base of the crust, with a limiting wave luminosity of $\sim 5 \times 10^{36}$ ergs s^{-1} at the same age. A wide range of $L_{\rm A}/L_{\rm X}$ is possible since, by coincidence, the core flux density that decays at an age of $\sim 10^4$ yr is very close to the flux density at which Hall transport in the crust switches from multiple fracturing to a plastic deformation. Magnetars are self-triggering burst sources, and no external impact or mass accretion is required.

Although the X-ray pulsar 1E 2259+586 (and its fellow AXPs) shares only secondary properties with the March 5 source and has never been seen to burst, its relative proximity (a factor ~20 closer in distance) makes it an important target for testing models of the SGRs. The absence of detected binary modulation, an optical companion (down to $V \sim 23$: Davies & Coe 1990) or quiescent radio emission (Coe et al. 1994) suggests that if this source is an accretor, then it is a very strange one: perhaps surrounded by an accretion disk but without any stellar companion (Corbet et al. 1995; Brandt & Podsiadlowski 1995; Van Paradijs et al. 1995; Duncan & Thompson 1994). If the accretion disk is acquired when the newly formed neutron star is kicked toward a stellar companion, then the characteristic radius of the disk at formation is $\sim GM_{ns}/V_{\rm kick}^2 \sim 0.3\ R_\odot\ (V_{\rm kick}/10^3\ {\rm km\ s^{-1}})^{-2}$, assuming that the density gradient scale inside the stellar companion is comparable. Letting $R_{\rm eff}$ be the radius at which the effective temperature of the disk is comparable to that of the Sun, the reflection luminosity in the visible band is

$$L_{\rm opt} \sim \frac{1}{2}\,L_\odot \left(\frac{R_{\rm eff}}{R_\odot}\right)^2 . \quad (98)$$

Equivalently, if a fraction f of the X-ray luminosity $L_{\rm X} \simeq (10$–$20)\ L_\odot$ is reprocessed to optical emission by the disk, then $R_{\rm eff}/R_\odot \sim (4$–$6) f^{1/2}$. If 1E 2259+586 is surrounded by an accretion disk, then this secondary optical emission should be detectable, with a periodic modulation of 7 s.[15] Alternatively, if such emission is not detected, then the identification of 1E 2259+586 with a strong-field neutron star ($B_{\rm dipole} \sim 0.7 \times 10^{14}$ G from the observed spin-down rate: TD93a, TD93b) is strongly suggested.

The nondetection of bursts from the AXPs is not surprising in this model. Their soft X-ray spectra and low particle emissivity suggests a greater similarity with SGR 0526−66 than with SGR 1806−20, and SGR 0526−66 has not been active as a burst source except for the 4 yr interval 1979–1983. Nonetheless, the identification of the AXPs with isolated magnetars leads to the prediction that these sources will eventually emit SGR bursts and perhaps extremely luminous superbursts similar to the March 5 event.

One of us (C. T.) would like to thank Charles Evans for discussions, Bohdan Paczyński for pointing out his paper on 1E 2259+586, Lars Bildsten for pointing out the source 1E 1048.1−5937, and Martin Rees and the Institute of

[14] On a timescale less than or comparable to the Alfvén crossing time of the star.

[15] The current upper bound on the optical flux (Davies & Coe 1990), after accounting for extinction, lies a factor ~10 below that expected from a low-mass X-ray binary of comparable $L_{\rm X}$ (Baykal & Swank 1996). Optical observations of SGR 0526−66 have the advantage of the much lower extinction toward the LMC but the disadvantage of the factor 20 increase in distance. Subtracting the estimated extinction of $A_v = 2.5$ toward 1E 2259+586 and taking into account the factor of 10 larger $L_{\rm X}$ (which corresponds to a factor of 3 larger optical luminosity for a typical LMXB: Van Paradijs & McClintock 1994), we estimate that observations of SGR 0526−66 would have to reach a limiting magnitude of $V = 26$ to obtain comparable sensitivity to optical reprocessing by an accretion disk.

Astronomy for their hospitality while part of this paper was written. R. C. D. thanks Cole Hellier for discussions. We would also like to thank the referee Shri Kulkarni for suggesting improvements in the discussion of the observations. A preliminary account of this work was presented by C. T. at the 1994 April APS meeting in Washington D.C.

This work was supported by the NASA Theoretical Astrophysics Program, grant NAG5-2773; by NASA grant NAG5-3100; by the NSERC of Canada; and by the Texas Advanced Research Program, grant ARP-279.

APPENDIX A

PARTICLE LUMINOSITY OF SGR 1806−20

Consider a supernova remnant of angular radius θ at a distance D. The synchrotron flux F_ν integrated over the remnant has a power-law spectrum $F_\nu \propto \nu^{-\alpha}$. We choose the distribution of the radiating electrons to be a power law in *momentum*

$$\frac{dn}{dp} = \frac{n_0}{m_e c}\left(\frac{p}{m_e c}\right)^{-\Gamma} \tag{A1}$$

(per unit volume). According to standard theory (see, e.g., Rybicki & Lightman 1979),

$$\alpha = \frac{\Gamma - 1}{2}\,. \tag{A2}$$

A key point is that, when the radio spectrum is steeper than $-\alpha = -0.5$, the kinetic energy density of the radiating electrons

$$U_e \propto p^2 \frac{dn}{dp} \propto p^{1-2\alpha} \quad (p \gg m_e c)\,, \tag{A3}$$

is dominated by mildly relativistic electrons. This is the case for the synchrotron nebula surrounding SGR 1806−20, where $-\alpha \simeq -0.6$ (Kulkarni & Frail 1993). The electron energy density is sensitive to a high-energy cutoff (spectral break energy) only when the radio spectrum is *harder* than $-\alpha = -0.5$, as it is in most radio plerions surrounding young active pulsars. Thus, the estimate of the electron energy density in SNR G10.0−0.3 given by Kulkarni & Frail (1993) is a slight overestimate.

The synchrotron emissivity (per unit volume and frequency) can be written as

$$\epsilon_\nu = \sqrt{3}\,\frac{\Gamma[(\Gamma/4) + (19/12)]\Gamma[(\Gamma/4) - (1/12)]k_2(\Gamma)}{(\Gamma + 1)k_1(\Gamma)}\,\frac{e^3 U_e B}{m_e^2 c^4}\left(\frac{2\pi m_e c\nu}{3eB}\right)^{-(\Gamma-1)/2}, \tag{A4}$$

where the total electron kinetic energy density

$$U_e = \left[\int_0^\infty (\sqrt{x^2+1} - 1)x^{-\Gamma}\,dx\right] n_0 m_e c^2 \equiv k_1(\Gamma) n_0 m_e c^2\,, \tag{A5}$$

$$k_2(\Gamma) \equiv \tfrac{1}{2}\int_0^\pi \sin^{(\Gamma+3)/2}\alpha\,d\alpha\,, \tag{A6}$$

and $\Gamma[\,]$ is the gamma function. Since $\epsilon_\nu \propto U_e(B^2/8\pi)^{(\Gamma+1)/4} \propto U_e(U - U_e)^{(\Gamma+1)/4}$, the combined energy density U of electrons and magnetic field is minimized when

$$U_e = \frac{4}{\Gamma + 5}\,U; \qquad \frac{B^2}{8\pi} = \frac{\Gamma + 1}{\Gamma + 5}\,U\,. \tag{A7}$$

Substituting $\Gamma = 2.4$ as appropriate to SNR G10.0−0.3, one finds

$$\epsilon_\nu = 0.87\,\frac{m_e \nu^3}{c}\left(\frac{U_{\rm min}\,e^2}{m_e^2 c^2 \nu^2}\right)^{1.85}. \tag{A8}$$

Using the relation $\epsilon_\nu = 3F_\nu/\theta^3 D$ and the observed 300 MHz flux of $F_\nu = 3.3 \times 10^{-23}$ ergs cm^{-2} Hz (Kulkarni & Frail 1993), one finds the particle energy

$$E_{\rm particle} = \frac{4}{\Gamma + 5}\,U_{\rm min}\,\frac{4\pi}{3}\,(\theta D)^3 = 1.7 \times 10^{48}\left(\frac{\theta}{2'.5}\right)^{1.38}\left(\frac{D}{8\ {\rm kpc}}\right)^{2.46}\ {\rm ergs}\,. \tag{A9}$$

The corresponding particle luminosity is

$$L_{\rm particle} = 5 \times 10^{36}\left(\frac{t}{10^4\ {\rm yr}}\right)^{-1}\left(\frac{\theta}{2'.5}\right)^{1.38}\left(\frac{D}{8\ {\rm kpc}}\right)^{2.46}\ {\rm ergs\ s^{-1}}\,. \tag{A10}$$

This value of $L_{\rm particle}$ was derived under the assumption that the electron spectrum (eq. [A1]) does not have a low-energy cutoff. Such a cutoff, if it exists, must be low enough that the synchrotron frequency at the cutoff lies below the lowest observing frequency $\nu_{\min}$. Equivalently, the Lorentz factor at the low energy cutoff is

$$\gamma_{e,\min} \lesssim \left(\frac{2\pi\nu_{\min} m_e c}{eB}\right) = 1 \times 10^3 \left(\frac{\nu_{\min}}{300\ \mathrm{MHz}}\right)^{1/3} \left(\frac{B}{10^{-4}\ \mathrm{G}}\right)^{-1/2}, \tag{A11}$$

where B is the magnetic field strength in the SNR. The integrated electron energy density scales down by a factor $\sim \gamma_{e,\min}^{2-\Gamma}$, and so in the case of SNR G10.0−0.3 (for which $\nu_{\min} = 300$ MHz) equations (A9) and (A10) overestimate the true value by at most $\sim 16(B/10^{-4}\mathrm{G})^{0.4}$.

APPENDIX B

PROPER MOTIONS OF THE AXPs

Given the large displacement of SGR 0526−66 from the center of the LMC supernova remnant N49 (Cline 1982), which implies a large proper motion of 1200 ± 300 km s^{-1} (DT92; Rothschild et al. 1994), it is natural to try to estimate proper motions for the AXP sources. From the X-ray and radio observations of Gregory et al. (1983), as interpreted in the SNR model of Wang et al. (1992), we infer that 1E 2259+586 is displaced 3.′1 to the east of the center of its associated SNR; this implies a transverse velocity $V_{\mathrm{trans}} \simeq 340(D/5\ \mathrm{kpc})$ km s^{-1}. The recoil of RXJ 1836−0301 is more difficult to estimate because of the irregular shape of the remnant (Schwentker 1994); however, it is clear that the star is significantly displaced, by $\sim 20'$, to the southeast of the centroid of the X-ray emissions. This gives a rough first estimate $V_{\mathrm{trans}} \sim 600(D/3\ \mathrm{kpc})$ km s^{-1}, using the SNR age estimate quoted in Table 1. These velocities are large enough to unbind the neutron stars from low-mass companions, but they do not preclude the possibility that AXPs are accreting from fossil disks (Corbet et al. 1995; van Paradijs et al. 1995; Duncan &Thompson 1994). Note that if AXPs are magnetars, a number of possible mechanisms exist for imparting a large proper motion to them at birth (DT92).

REFERENCES

Baykal, A., & Swank, J. 1996, ApJ, 460, 470
Baym, G., Pethick, C., & Pines, D. 1969, Nature, 224, 674
Bhattacharya, D., & van den Heuvel, E. P. J. 1991, Phys. Rep., 203, 1
Blaes, O., Blandford, R., Goldreich, P., & Madau, P. 1989, ApJ, 343, 829
Blair, W. P., & Kirshner, R. P. 1981, Nature, 291, 132
Brandt, N., & Podsiadlowski, P. 1995, MNRAS, 274, 461
Cline, T. L. 1982, in Gamma Ray Transients and Related Astrophysical Phenomena, ed. R. E. Lingenfelter et al. (New York: AIP), 17
Coe, M. J., Jones, L. R., & Lehto, H. 1994, MNRAS, 270, 178
Corbet, R. H. D., & Day, C. S. R. 1990, MNRAS, 243, 553
Corbet, R. H. D., Smale, A. P., Ozaki, M., Koyama, K., & Iwasawa, K. 1995, ApJ, 433, 786
Davies, S. R., & Coe, M. J. 1990, MNRAS, 245, 268
Duncan, R. C., Li, H., & Thompson, C. 1993, in Compton Gamma Ray Observatory, ed. M. Friedlander, N. Gehrels, & R. J. Macomb (New York: AIP), 1074
Duncan, R. C., & Thompson C. 1992, ApJ, 392, L9 (DT92)
———. 1994, in Gamma-Ray Bursts, ed. G. J. Fishman, J. J. Brainerd, & K. Hurley (New York: AIP), 625
———. 1995, in High-Velocity Neutron Stars and Gamma-Ray Bursts, ed. R. E. Rothschild & R. E. Lingenfelter (New York: AIP), in press (DT95)
Easson, I., & Pethick, C. J. 1977, Phys. Rev. D, 16, 275
Fenimore, E. E., Laros, J. G., & Ulmer, A. 1994, ApJ, 432, 742
Flowers, E., & Ruderman, M. 1977, ApJ, 395, 302
Friman, B. L., & Maxwell, O. V. 1979, ApJ, 232, 541
Goldreich, P., & Reisenegger, A. 1992, ApJ, 395, 250 (GR92)
Gregory, P. C., & Fahlman, G. G. 1980, Nature, 287, 805
Gregory, P. C., et al. 1983, in Supernova Remnants and Their X-Ray Emissions, ed. J. Danziger & P. Gorenstein (Dordrecht: Reidel), 437
Hellier, C. 1994, MNRAS, 271, L21
Hernquist, L. 1985, MNRAS, 213, 313
Hoffberg, M., Glassgold, A. E., Richardson, R. W., & Ruderman, M. A. 1970, Phys. Rev. Lett., 24, 775
Hurley, K., McBreen, B., Rabbette, M., & Steel, S. 1994a, A&A, 288, L49
Hurley, K., Sommer, M., Kouveliotou, C., Fishman, G., Meegan, C., Cline, T., Boer, M., & Niel, M. 1994b, ApJ, 431, L31
Israel, G. L., Mereghetti, S., & Stella, L. 1994, ApJ, 433, L25
Iwasawa, K., Koyama K., & Halpern J. P. 1992, PASJ, 44, 9
Jones, P. B. 1988, MNRAS, 233, 875
Joss, P. C., & Li, F. K. 1980, ApJ, 238, 287
Kaplan, D. B., & Nelson, A. E. 1986, Phys. Lett., B175, 57
Kingsep, A. S., Chukbar, K. V., & Yan'kov, V. V. 1990, Rev. Plasma Phys., 16, 243
Kulkarni, S. R. 1992, Philos. Trans. R. Soc. London, A, 341, 77
Kulkarni, S. R., & Frail, D. A. 1993, Nature, 365, 33
Kulkarni, S. R., Frail, D. A., Kassim, N. E., Murakami, T., & Vasisht, G. 1994, Nature, 368, 129
Kulkarni, S. R., Matthews, K., Neugebauer, G., Reid, I. N., van Kerkwijk, M. H., & Vasisht, G. 1995, ApJ, 440, L61
Laros, J. G., et al. 1987, ApJ, 320, L111
Li, H., & Dermer, C. D. 1992, Nature, 359, 514
Link, B., & Epstein, R. I. 1995, preprint
Lohsen, E. H. G. 1981, ApJS, 44, 1
Lorenz, C. P., Ravenhall, D. G., & Pethick, C. J. 1993, Phys. Rev. Lett., 70, 379
Mazets, E. P., Golenetskii, S. V., Guryan, Yu. A., & Ilyinskii, V. N. 1982, Ap&SS, 84, 173
Mereghetti, S., Caraveo, P., & Bignami, G. F. 1992, A&A, 263, 172
Mereghetti, S., & Stella, L. 1995, ApJ, 422, L17
Mészáros, P., Rees, M. J., & Papathanassiou, H. 1994, ApJ, 432, 181
Morini, M., Robba, N. R., Smith, A., & van der Klis, M. 1988, ApJ, 333, 777
Murakami, T., Tanaka, Y., Kulkarni, S. R., Ogasaka, Y., Sonobe, T., Ogawara, Y., Aoki, T., & Yoshida, A. 1994, Nature, 368, 127
Norris, J. P., Hertz, P., Wood, K. S., & Kouveliotou, C. 1991, ApJ, 366, 240
Pacini, F. 1967, Nature, 216, 567
Paczyński, B. 1990, ApJ, 365, L9
———. 1992, Acta Astron., 42, 145
Pethick, C. J. 1992, in Structure and Evolution of Neutron Stars, ed. D. Pines, R. Tanagaki, & S. Tsuruta (Redwood City: Addition-Wesley), 115
Pethick, C. J., & Thorsson, V. 1994, Phys. Rev. Lett., 72, 1964
Podsiadlowski, P., Rees, M. J., & Ruderman, M. A. 1995, MNRAS, 273, 755
Reisenegger, A., & Goldreich, P. 1992, ApJ, 395, 240
Rothschild, R. E., Kulkarni, S. R., & Lingenfelter, R. E. 1994, Nature, 368, 432
Rothschild, R. E., Lingenfelter, R. E., Seward, F. D., & Vancura, O. 1993, in Compton Gamma Ray Observatory, ed. M. Friedlander, N. Gehrels, & R. J. Macomb (New York: AIP), 808
Ruderman, M. A. 1991, ApJ, 382, 587
Rybicki, G. B., & Lightman, A. P. 1979, Radiative Processes in Astrophysics (New York: Wiley)
Sauls, J. A., & Serene, J. W. 1978, Phys. Rev. D, 17, 1524
Sawyer, R. F. 1989, Phys. Rev. D, 39, 3804
Schmidt, G. D., & Smith, P. S. 1995, ApJ, 488, 305
Schwentker, O. 1994, A&A, 286, L47
Seward, F. D., Charles, P. A., & Smale, A. P. 1986, ApJ, 305, 814
Shalybkov, D. A., & Urpin, V. A. 1995, MNRAS, 273, 643
Shapiro, S. L., & Teukolsky, S. A. 1983, Black Holes, White Dwarfs, and Neutron Stars (New York: John Wiley & Sons)
Sonobe, T., Murakami, T., Kulkarni, S. R., Aoki, T., & Yoshida, A. 1994, ApJ, 436, L23
Stenle, H., Pietsch, W., Gottwald, M., & Graser, U. 1987, Ap&SS, 131, 687
Takatsuka, T. 1972, Prog. Theoret. Phys., 48, 1517
Tayler, R. J. 1973, MNRAS, 161, 365
Thompson, C., & Duncan, R. C. 1993a, ApJ, 408, 194 (TD93a)
———. 1993b, in Compton Gamma Ray Observatory, ed. M. Friedlander, N. Gehrels, & R. J. Macomb (New York: AIP), 1085 (TD93b)
———. 1995, MNRAS, 275, 255 (TD95)
Tsuruta, S. 1995, in The Lives of the Neutron Stars, ed. M. A. Alpar et al. (Dordrecht: Kluwer), 133
Ulmer, A., Fenimore, E. E., Epstein, R. I., Ho, C., Klebesadel, R. W., Laros, J. G., & Delgado, F. 1993, ApJ, 418, 395
Urpin, V. A., & Ray, A. 1994, MNRAS, 267, 1000

Urpin, V. A., & Shalybkov, D. A. 1995, A&A, 294, 117
Urpin V. A., & Yakolev, D. G. 1980, Soviet. Astron., 24, 126
Usov, V. V. 1984, Ap&SS, 107, 191
———. 1993, ApJ, 410, 761
———. 1994, ApJ, 427, 984
Van Kerkwijk, M. H., Kulkarni, S. R., Matthews, K., & Neugebauer, G. 1995, ApJ, 444, L33
Van Paradijs, J., & McClintock, J. E. 1994, A&A, 290, 133.
Van Paradijs, J., Taam, R. E., & van den Heuvel, E. P. J. 1995, A&A, 299, 41
Van Riper, K. A. 1988, ApJ, 329, 339
———. 1991, ApJ, 372, 251
Van Riper, K. A., Epstein, R. I., & Miller, G. S. 1991, ApJ, 381, L47
Vancura, O., Blair, W. P., Long, K. S., & Raymond, J. C. 1992, ApJ, 394, 158
Vasisht, G., Frail, D. A., & Kulkarni, S. R. 1995, ApJ, 440, L65
Vasisht, G., Kulkarni, S. R., Frail, D. A., & Greiner, J. 1994, ApJ, 431, L35
Verbunt, F. 1990, in Neutron Stars and Their Birth Events, ed. W. Kundt (Dordrecht: Kluwer), 179
Wang, Z., Qu, Q., Luo, D., McCray, R., & Mac Low, M. 1992, ApJ, 388, 127
Yakovlev, D. G., & Shalybkov, D. A. 1990, Soviet Astron. Lett., 16, 86
Zahn, J.-P. 1989, A&A, 220, 112